

Boundary-layer instability noise on aerofoils

By EMMA C. NASH¹, MARTIN V. LOWSON¹
AND ALAN McALPINE²

¹Department of Aerospace Engineering, University of Bristol, Bristol BS8 1TR, UK

²School of Mathematics, University of Bristol, Bristol BS8 1TR, UK

(Received 12 February 1998 and in revised form 28 September 1998)

An experimental and theoretical investigation has been carried out to understand the tonal noise generation mechanism on aerofoils at moderate Reynolds number. Experiments were conducted on a NACA0012 aerofoil section in a low-turbulence closed working section wind tunnel. Narrow band acoustic tones were observed up to 40 dB above background noise. The ladder structure of these tones was eliminated by modifying the tunnel to approximate to anechoic conditions. High-resolution flow velocity measurements have been made with a three-component laser-Doppler anemometer (LDA) which have revealed the presence of strongly amplified boundary-layer instabilities in a region of separated shear flow just upstream of the pressure surface trailing edge, which match the frequency of the acoustic tones. Flow visualization experiments have shown these instabilities to roll up to form a regular Kármán-type vortex street.

A new mechanism for tonal noise generation has been proposed, based on the growth of Tollmien–Schlichting (T–S) instability waves strongly amplified by inflectional profiles in the separating laminar shear layer on the pressure surface of the aerofoil. The growth of fixed frequency, spatially growing boundary-layer instability waves propagating over the aerofoil pressure surface has been calculated using experimentally obtained boundary-layer characteristics. The effect of boundary-layer separation has been incorporated into the model. Frequency selection and prediction of T–S waves are in remarkably good agreement with experimental data.

1. Introduction

Tonal noise generation has been found to be a prevalent problem on aerofoils operating at moderate Reynolds numbers ($100\,000 < Re_c < 2\,000\,000$) and has been observed to occur on wind turbines, small aircraft, gliders, fans and rotors, and has more general interest as a model problem for airframe noise radiation. Such tonal noise may well have been present on the original Wright Flyer. British journalist Harry Harper reported in 1908 (cf. Howard 1987):

What one did hear quite clearly was an odd sort of chattering, clattering sound from the crossed chains which drove the long bladed air-screws. And there was a penetrating whistling sound from the air-screws themselves. The net result was a mingled whistling, chattering hum which, once heard, could never be forgotten.

Classically, discrete frequencies from aerodynamic sources are associated with the Kármán vortex street. Indeed, in the early part of the century this was regarded as the principal cause of drag production by many investigators. In more modern times, the significance of the Kármán vortex street on the flows on streamline bodies

such as aerofoils has been de-emphasized, and transition processes have been seen as the dominant issue. Kármán vortex streets remain a critical part of bluff-body flow structures, and are also a well-known source of discrete frequency noise in aeolian tones. However, Kármán vortex streets on aerofoils are normally associated with relatively low Reynolds numbers typically below 100 000, or with blunt trailing edges, e.g., Brooks, Pope & Marcolini (1989).

The first clear identification of discrete frequency tones from a sharp-trailing-edge aerofoil at moderate Re appears to be due to Clark (1971), although no detailed analysis of these peak frequencies was carried out. Hersh & Hayden (1971) made similar observations of discrete acoustic tones generated by a NACA0012 aerofoil section and a two-bladed propeller in smooth flow at Reynolds numbers based on chord up to 330 000. Hersh & Hayden believed that the discrete frequencies were due to a laminar separation at the leading edge of the aerofoil and used leading-edge serrations to control the effect.

Paterson *et al.* (1973) carried out the first detailed investigation of tonal noise emitted by NACA0012 and NACA0018 aerofoil sections in a Reynolds number range corresponding to full-scale helicopter rotors. These studies were undertaken in an anechoic open jet wind tunnel. They used the laminar boundary-layer formula for a flat plate in zero pressure gradient to suggest the following scaling law:

$$f = KU^{1.5}/(cv)^{0.5}, \quad (1)$$

where f = frequency of acoustic tone, U = free-stream velocity, c = chord length, ν = kinematic viscosity, and K = an arbitrary constant.

A key finding in Paterson *et al.* was that within the overall $U^{1.5}$ frequency dependence there was a ladder-like frequency structure with each 'rung' of the ladder varying in frequency as $U^{0.8}$. The constant K in equation (1) giving the best fit with the data was found to be 0.011, and gave a characteristic Strouhal number based on boundary-layer thickness at the trailing edge of around 0.11. Equivalent results have been found in a number of subsequent investigations.

Paterson *et al.* found that the velocity range over which tonal noise was present increased with incidence until the aerofoil stalled. This was attributed to the adverse pressure gradient becoming less severe at the pressure surface trailing edge with increased incidence, thereby maintaining laminar flow to the trailing edge at higher velocities. Intensity of the tone increased with velocity, reached a plateau, then decreased before disappearing. Noise levels were found to decrease in a transition region associated with gradual turbulent transition on the pressure surface of the aerofoil. As first found by Hersh & Hayden (1971), all noise disappeared when a trip wire was placed forward of 80 per cent chord in the laminar boundary layer. It was inferred by Paterson *et al.* that discrete frequencies can be radiated from an aerofoil when a laminar boundary layer extends to the trailing edge of one surface. It was also observed that tonal noise was no longer observed at flow conditions predicted as being transitional to turbulence. However, it was not confirmed that tonal noise disappeared at high Reynolds numbers, only that if it did exist, it was lower in intensity than the open jet background noise.

Paterson *et al.* (1973), and also Sunyach *et al.* (1973), concluded from correlation measurements between the aerofoil boundary layer and a far-field microphone that the acoustic field of the aerofoil was governed by vortex-shedding phenomenon at the trailing edge of the aerofoil. Later Schlinker, Fink & Amiet (1976) and Munin, Prozorov & Toporov (1992) carried out correlation measurements with a directional microphone and confirmed that noise was generated at the trailing edge and was

dipole in nature. Munin *et al.* also investigated the influence of free-stream velocity and turbulence level on noise levels. It was found that as free-stream velocity and turbulence increased, tones diminished in strength and eventually disappeared.

Tam (1974) argued that the acoustic tones observed were unrelated to vortex shedding because vortex shedding could not explain the characteristic features associated with the discrete tone phenomenon. In addition, Tam pointed out that the wake from a streamlined body would form vortices, initiated by wake instabilities, at a substantial distance from the trailing edge. It was therefore difficult to associate these vortices with the noise source of the discrete tone which is known to be near the trailing edge. Instead, Tam proposed that tonal noise produced was due to a self-excited feedback loop formed by an acoustic field, the boundary layer and the wake of the aerofoil.

According to the above feedback model, disturbances are continuously initiated at the sharp trailing edge of the aerofoil. Tam was the first to propose that the aerodynamic source of these disturbances was Tollmien–Schlichting (T–S) instability waves, and showed that almost all the frequencies measured by Paterson *et al.* (1973) lay between the upper and lower branches of the neutral stability curve calculated by Lin (1995) and Shen (1954) for a flat plate, discrepancies being ascribed to the existence of a pressure gradient. Tam also suggested that these effects would be moderated by aeroacoustic feedback processes.

Fink, Schlinker & Amiet (1976) published another account of experimental research into the generation of tonal noise. Measurements were conducted in an acoustic open jet wind tunnel on NACA0012 aerofoils. Constant-chord and tapered-chord models were tested. The constant-chord model was observed to generate discrete multiple tones which were several hundred Hertz apart. This was thought to be due to spanwise irregularities in the wing, which had a long span to chord ratio of 6.89. The tapered chord models also radiated discrete multiple tones, but there were more tones, over a wider frequency range than from the constant chord model. The variation of the sound pressure level of the strongest tones with increased velocity agreed with that of Paterson *et al.* (1973) and was found to increase in strength with velocity to the fifth power, reach a plateau, then decay. Fink *et al.* also proposed a theoretical model for the T–S instability process which gave limited agreement with the experimental data. This was later developed by Fink (1978) to provide a description of the proposed feedback process.

Wright (1976) investigated both discrete and broadband noise produced by a wide range of rotor types, including helicopter rotors, propellers and fans. Noise associated with T–S instabilities was found to be most apparent for blades at low angles of incidence, operating at low speeds and having small chord lengths and large thickness to chord ratios. The tonal frequencies observed were shown to take the form of a single narrow-band discrete peak, a series of discrete peaks or, most commonly, a broad continuous spectral peak. Wright proposed an aeroacoustic feedback loop between the trailing edge of the aerofoil, which acts as the radiation point, and a region upstream on the aerofoil surface, which acts as the source. Wright assumed that the boundary layer remains effectively laminar to the trailing edge. The proposed mechanism was that wave disturbances in the laminar boundary layer convect along the aerofoil surface to the trailing edge. The boundary-layer waves induce a pressure disturbance on leaving the aerofoil surface at the trailing edge. The resulting radiation then propagates upstream to reinforce their original disturbance thus completing a feedback loop.

Longhouse (1977) investigated the vortex-shedding noise of axial flow fans. He carried out extensive flow-visualization experiments using acenaphthalene coating

to compare the level and type of noise emission with the state of the boundary layer on the blade. Longhouse tested three-dimensional cambered wing sections that produced many tonal peaks at each velocity. To reduce the number of peaks produced, Longhouse fitted a serrated strip to the blade leaving a small spanwise gap which approximated the untripped region to a two-dimensional wing, and which enabled the vortex-shedding noise to be related to a known Reynolds number. Owing to the cambered shape of the wing sections, the laminar flow surface was the suction surface.

The flow-visualization experiments indicated that for vortex shedding to occur, the boundary layer had to be laminar to the trailing edge. The point at which vortex-shedding noise ceased coincided with the point at which the flow became turbulent at the trailing edge. An experiment to confirm this result was to extend the chord length of a blade section by 4.8 mm at its trailing edge, i.e. by 8.4% of the original chord length. Testing at a fixed velocity had originally produced vortex-shedding noise with laminar flow to the trailing edge. At the same velocity, the now extended blade was turbulent at the trailing edge, resulting in the disappearance of any vortex-shedding noise. Longhouse also found that a serrated leading edge which tripped the flow to be turbulent at the trailing edge eliminated tonal noise emission.

Longhouse suggested that the beginning of laminar boundary-layer instabilities must be sufficiently upstream of the trailing edge for natural amplification to occur. The acoustic noise would therefore be expected to be loudest when natural transition is just about to occur at the trailing edge. He also pointed out that the presence of an adverse pressure gradient, such as that present on an aerofoil, would produce the strong amplification of the instabilities required. As part of his evaluation of the feedback processes Longhouse calculated boundary-layer profiles around the blades. These showed the existence of laminar separation bubbles which had gone undetected in experiment, which would be expected to have significant effects on the amplification and feedback process. However, he did not develop this argument further.

Arbey & Bataille (1983) undertook an experimental and theoretical study of a NACA0012 aerofoil. They postulated that T-S waves initiated broadband noise when diffracted around the trailing edge of the aerofoil, which then triggered a feedback loop as described by Wright (1976), Longhouse (1977) and Fink (1978). The peaks, f_n were spaced at regular intervals of 110 Hz and followed a $U^{0.85}$ dependence whereas the frequency pattern as a whole was found to follow a $U^{1.5}$ dependence, i.e. results parallel to those found by Paterson *et al.* Arbey & Bataille derived an empirical prediction equation which coincides with Paterson's $U^{1.5}$ law for central peak tone frequencies.

Akishita (1986) questioned whether discrete tonal frequencies produced by an aerofoil in laminar flow could be produced from laminar instabilities alone, since the latter are continuous and broadband in nature. He argued that frequency discretizing requires a frequency selection mechanism. The effect of a trip strip placed on the suction, i.e. turbulent, side of a NACA0015 aerofoil was investigated. Akishita claimed that there was no effect on noise until the trip was placed at the trailing edge, at which point any tonal noise disappeared. Akishita found that measured values of flow turbulence at various positions within the wake had two peaks, above and below the aerofoil. The velocity profile of the pressure side of the wing at the trailing edge indicated that the flow was laminar to the trailing edge. However, the value of flow turbulence 1 mm behind the trailing edge was extremely high. Akishita inferred from these results that the flow turbulence on the pressure side of the aerofoil is induced from the suction side turbulent boundary layer. The feedback loop mechanism proposed by Akishita was that a sound wave is generated in the wake just downstream from the trailing edge owing to laminar instabilities on the pressure surface.

Thus, at the commencement of the present work there had been a number of studies of aerofoil discrete tones. The majority of researchers found their results agreed with the original results of Paterson *et al.* (1973). Most workers found that the tones were related to a laminar boundary layer on the pressure surface of the aerofoil, and that the tones were eliminated by tripping the pressure surface boundary layer sufficiently far upstream of the trailing edge ($< 80\%$ chord). The importance of the T-S instability process was also recognized following the work of Tam (1974). However, the fact that T-S waves first appear at much lower Reynolds numbers than the associated noise remained anomalous. Most workers also emphasized the essential contributions of a feedback loop in the determination of the discrete frequencies, although details of the ladder process appeared to vary considerably in different experiments and several feedback formulae were available, giving rather different results. Thus, significant progress had been made in understanding the mechanism behind tonal noise generation, but many experimental observations remain unexplained.

The most significant shortcoming of the previous research was the failure to recognize the importance of the long laminar separation bubble that is a feature of the flow on the aerofoil pressure surface at modest Re . Indeed, the majority of papers have explicitly assumed that the flow on at least one surface of the aerofoil is laminar to the trailing edge. In the presence of separation just ahead of the trailing edge, this is unlikely. The existence of a separated boundary layer at the trailing edge would also cast doubt on some of the frequency prediction expressions (Paterson *et al.* 1973; Fink *et al.* 1976; Arbey & Bataille 1983), which use boundary-layer thickness parameters at the trailing edge assuming the flow to be over a flat plate, laminar and attached.

Initial work using a numerical boundary-layer prediction code written by S. P. Fiddes (private communication) showed that the separated laminar flow will appear on the pressure surface of a NACA0012 aerofoil over the range of Reynolds numbers and incidences for which tonal noise is known to be generated. This theoretical prediction was confirmed by extensive surface flow visualizations. This was first reported by Lawson, Fiddes & Nash (1994). The mechanism proposed in that paper, and further developed in the present paper, is based on a three part process, which is illustrated in figure 2. First, T-S instabilities develop in the laminar boundary layer on the pressure surface of the aerofoil; secondly, these frequencies are massively amplified by the inflectional profiles of the separating shear layer at the trailing edge; thirdly, the sound is radiated as these amplified instabilities pass the trailing edge. Thus, the tonal noise is controlled by large-scale instabilities associated with the separated shear flow near the aerofoil trailing edge. The work reported in the present paper has confirmed this basic mechanism, but shown further that the frequency selected is that which is the most amplified during the growth of the instability.

The present paper reports further results from an extensive study of tone generation on a NACA0012 aerofoil mounted in a closed wind tunnel. Initial results from the present study have been reported in Nash & Lawson (1995). The work described in the present paper has been carried out to confirm the importance of separating flow near the trailing edge as a condition for the generation of tonal noise. The significance of this flow, particularly in terms of influencing T-S instability waves has also been examined, with the aim of further understanding the tonal noise generation mechanism.

Most previous measurements of aerofoil noise have been carried out in open jet facilities. This is to eliminate the likely effects of hard wall resonances on the results. It is well established (Parker 1966, 1967), that cross-tunnel resonances can have dominant effects on the acoustic response in a wind tunnel. The principal Parker

beta mode response occurs at a frequency which is fixed by the tunnel cross-stream dimensions. Thus, it was believed possible to undertake useful measurements at frequencies remote from such effects. To reduce possible problems the tunnel was also acoustically lined.

This paper reports further work using analogue LDA results to provide information on the structure of the unsteady flow field over the aerofoil. This has been supported by new flow visualization results, and by a new theoretical model which examines the consequences of systematic application of classical boundary-layer instability theory. The measurements reported here were undertaken on a NACA0012 aerofoil. Further measurements and theoretical investigations have also been taken on NACA23015 and FX79 W151 aerofoils. These provided confirmation of all of the features reported in the present paper, but space does not permit discussion here. Fuller details are available in Nash (1996).

2. Experimental arrangements

All experimental work completed during the research programme was carried out in the closed-working-section, closed-loop, low-turbulence wind tunnel at the Department of Aerospace Engineering at Bristol University. A detailed description of this facility is given by Barrett (1984). The working section had a rectangular cross-section of $0.85 \text{ m} \times 0.6 \text{ m}$ and was 1.5 m long with corner fillets tapering from $141 \text{ mm} \times 106 \text{ mm}$ at entry to $123 \times 93 \text{ mm}$ at the exit. The flow quality in the wind tunnel was high, with negligible spatial variation of flow velocity to within 50 mm of the wind tunnel walls. The wind tunnel was designed to achieve turbulence intensities below 0.05% at 60 m s^{-1} .

The wind tunnel was driven by a 75 kW , 1500 r.p.m. d.c. motor with a thyristor control unit. Background acoustic measurements taken in the empty wind tunnel showed that peak frequencies of 600 and 900 Hz are intermittently apparent over the velocities of 10 m s^{-1} to 30 m s^{-1} . These were caused by the motor thyristor power unit and these frequencies were subsequently discounted from any acoustic measurements taken with the aerofoils installed. Additional intermittent peak frequencies above 4000 Hz between 40 m s^{-1} and 70 m s^{-1} were considered to be due to the presence of instability effects on the motor fan blades. These frequencies were above the range of frequencies under investigation, and were ignored.

The principal experiments were carried out on a NACA0012 profile of 0.3 m chord. This also gave an opportunity for direct comparison with previous work. The aerofoil was mounted horizontally across the wind tunnel, completely spanning the test section as shown in figure 1. This figure also shows the acoustic lining which was added to the tunnel for the majority of the tests reported here. An unobscured view of the aerofoil in the wind tunnel enabled laser-Doppler anemometer measurements to be taken. The experimental Reynolds number range, based on chord, was up to $1\,450\,000$, i.e. 71 m s^{-1} in the low-turbulence wind tunnel.

All acoustic measurements were made with a Brüel and Kjær (B & K) half-inch condenser microphone, Type 4134, which was shielded with a polished nose cone to reduce background wind noise. The microphone was attached to a probe mounted vertically through the wind tunnel ceiling, at a position approximately 100 mm behind the NACA0012 aerofoil trailing edge, midway between the trailing edge and wind tunnel ceiling and at midspan. The microphone was positioned downstream of the trailing edge, so as not to affect the flow over the aerofoil, and away from the wake to avoid detecting extraneous noise.

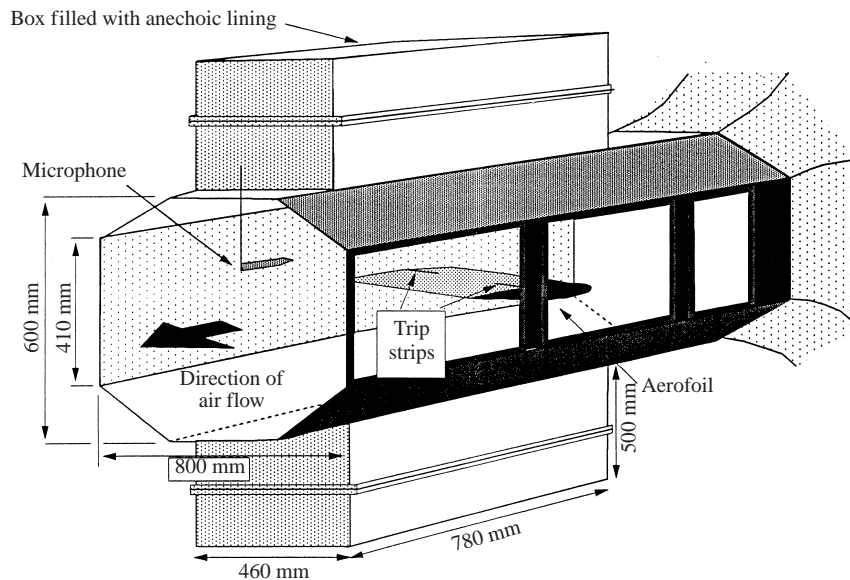


FIGURE 1. Modified working section of the low-turbulence wind tunnel.

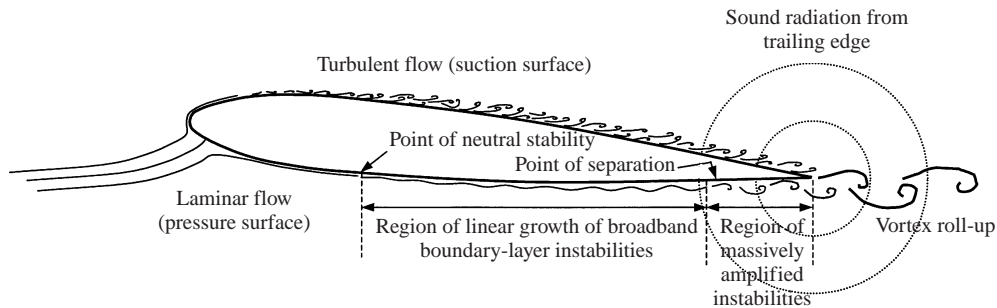


FIGURE 2. Diagram showing aerofoil flow processes.

Data analysis was achieved via B & K dual-channel, real-time frequency analyser Type 2144 which gave both $\frac{1}{24}$ octave and dual-channel, real-time FFT analysis. All of the data discussed herein were recorded on digital audio tape (DAT) for post-processing analysis.

3. Acoustic results on a NACA0012

3.1. Tests in an unlined tunnel

The first studies of tonal quality were undertaken directly in the hard-wall wind tunnel without acoustic lining. Initial studies on this aerofoil did not demonstrate any discrete frequency tones. This was found to be due to the slight roughness of the painted surface of the aerofoil. After rubbing down this surface to an extremely smooth finish, the aerofoil showed tonal acoustic response over a wide range of speeds and angles of attack.

It is surprising that the acoustic phenomena observed here have not been reported from other wind-tunnel tests conducted in a closed-working-section wind tunnel,

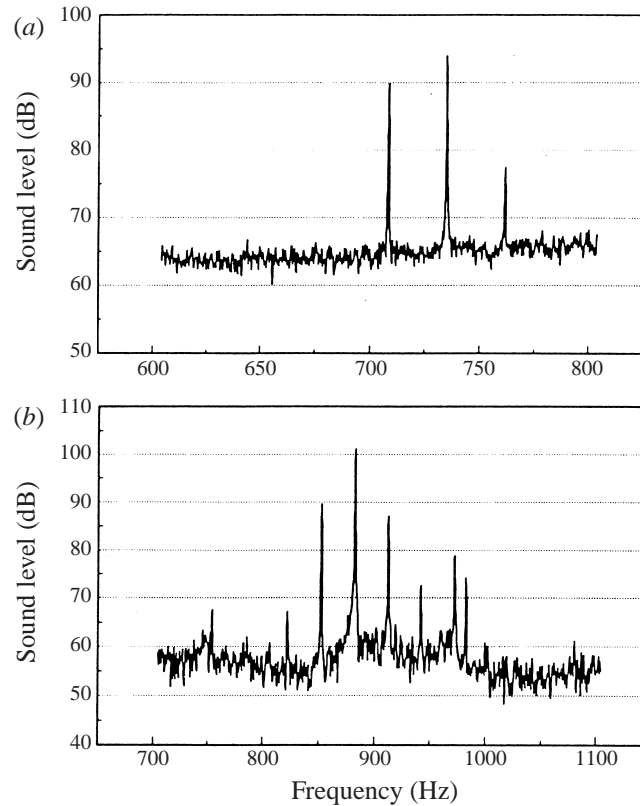


FIGURE 3. Typical frequency spectra—hard-wall tunnel. (a) Incidence = -3° , velocity = 23.4 m s^{-1} . (b) Incidence = -4° , velocity = 26.1 m s^{-1} .

particularly as the tonal noise is clearly audible. The size and speed of the present tests are typical of a great many tests carried out in small laboratory facilities. It seems certain that the acoustic behaviour must affect the transition process of the laminar boundary layer/separated shear layer. The present tests have shown that discrete frequency aerofoil noise always occurs at moderate Re provided both the flow and the aerofoil are sufficiently smooth. Thus, the absence of noise in any test would place doubt on the accuracy of the test set-up. A brief study was conducted on the influence of acoustic resonance on aerofoil drag for the NACA0012 aerofoil. This showed significant increases of drag due to the resonance process. Results from this study will be reported separately, and are also given in Nash (1996).

Figure 3 shows some typical frequency spectra measured in the hard-wall tunnel, revealing multiple frequency peaks of up to 40 dB above the background level, a few Hz in bandwidth. The frequency spectrum was found to be very sensitive to both tunnel speed and aerofoil angle of attack, but, despite its complexity, to be very repeatable. Figure 4 shows the structure of the peak tonal frequencies against wind-tunnel velocity. A comparison with the empirically derived prediction of Paterson *et al.* is also shown. Both the overall $U^{1.5}$ and local dependence on $U^{0.8}$ are found. However, the acoustic behaviour is strongly influenced by resonant frequencies which occur at 250, 540, 750 and to a lesser extent at 950 Hz. These were consistent with Parker beta mode resonant frequencies.

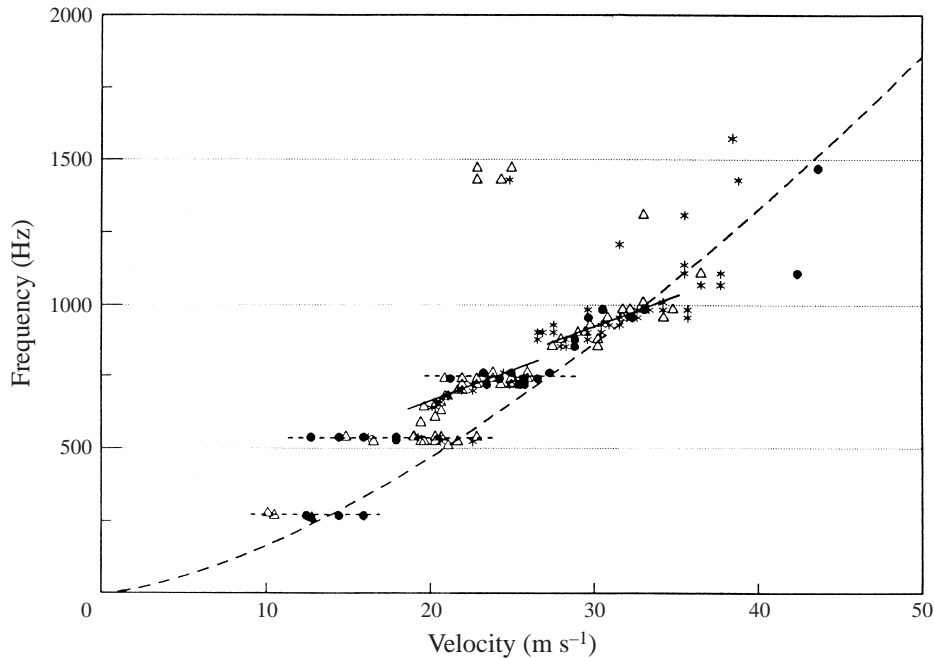


FIGURE 4. Peak frequencies versus velocity for hard-wall tunnel. Angle of attack \bullet , -2° ; \triangle , -3° ; $*$, -4° ; - - -, resonant frequencies; —, frequency $\propto U^{0.8}$; - · -, predicted (Paterson *et al.*).

The complex ladder structure for this hard-wall test is generally consistent with the results of other investigators, e.g. Paterson *et al.* (1973) and Arbey & Bataille (1983) in an open jet. However, Arbey & Bataille, for example, found that the frequencies were always spaced 110 Hz apart. Although some cases examined showed a uniform separation of frequency peaks there was little uniform pattern to the frequencies measured in the present experiments. It was thought that the results were likely to be influenced by the presence of the tunnel walls. Thus, a modification to the wind tunnel was made to approximate the working section to an anechoic environment.

3.2. Experiments in an acoustically lined tunnel

The tunnel test-section floor and ceiling were removed and replaced with two wooden boxes both $0.78 \text{ m} \times 0.46 \text{ m}$ and 0.5 m in depth that were filled with layers of 4 inch thick foam. It was sufficient to line only the working section of the wind tunnel with acoustic foam above and below the aerofoil. The wind-tunnel modification is shown in figure 1 where it can be seen that the sloped sides of the working-section floor and ceiling were not replaced with acoustic lining. These regions would have been extremely difficult to line because they formed the main structure of the working section, and also contained striplights.

The unlined fillets gave concern about unrepresentative response. The solution to this problem was to fit the aerofoil with trip strips on the outer portions of the blade, thus confining the instability process to the centre portion of the aerofoil where it would not be unduly affected by the wind-tunnel fillets, and producing a set-up which was close to two-dimensional. It was found that with both acoustic lining and side trips, the number of tones obtained at each velocity and incidence is much reduced, compared with the data obtained without acoustic lining. In addition to this, the Parker mode resonant frequencies are almost totally eliminated. It appears

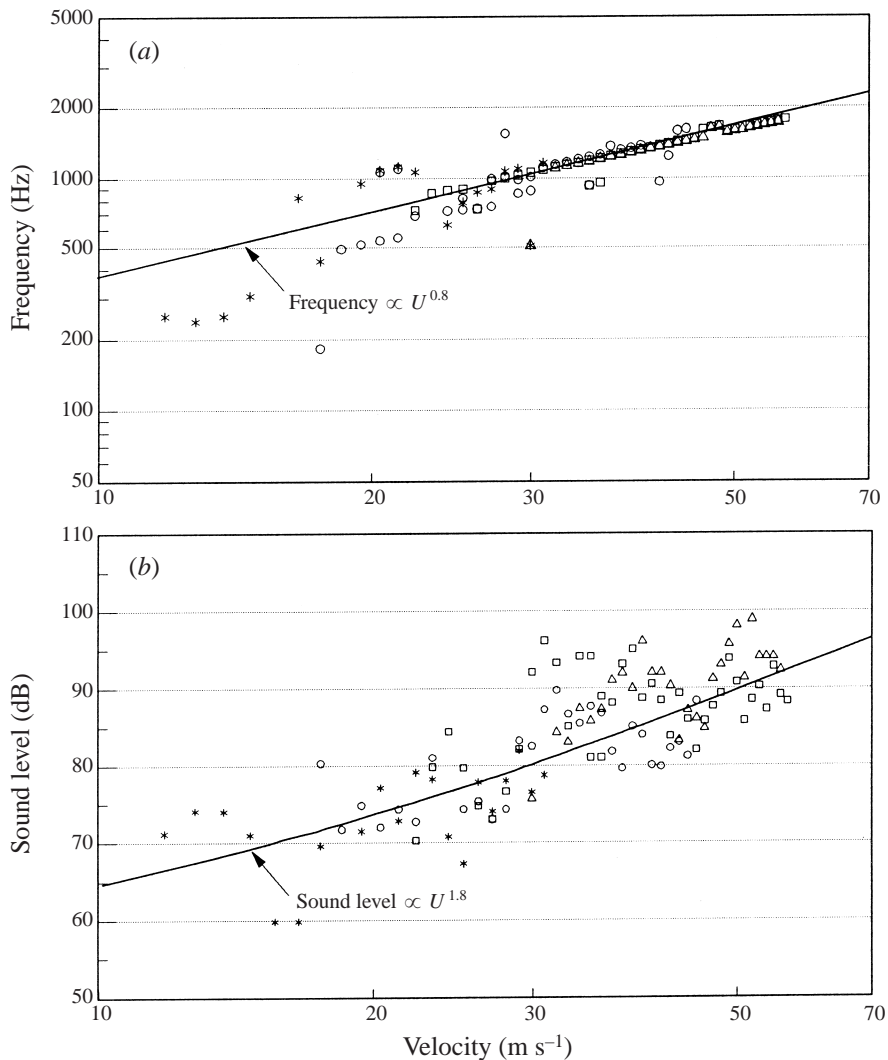


FIGURE 5. Frequencies and sound levels at all incidences quasi-anechoic tunnel.
 *, -2° ; O, -3° ; □, -4° ; Δ, -5° .

reasonable to assume that for the central portion of the aerofoil the working section is approximating to anechoic conditions.

Figure 5 shows the overall structure of the tones obtained under anechoic conditions at all incidences tested. At the majority of test cases, a single dominant tonal frequency was observed. The structure of the tones is extremely ordered, and repeatable, with the familiar $U^{0.8}$ dependence with velocity (Paterson *et al.* 1973). However, a major discrepancy with previous investigations such as those of Paterson *et al.*, Fink *et al.* (1976) and Arbey & Bataille (1983) is that there is no ladder-like structure of tonal 'jumps' with velocity.

The presence of frequency jumps indicates an integer increase in the number of wavelengths present in a feedback loop mechanism. The absence of frequency jumps implies that there was no feedback loop present for this series of experiments. However, the strength and narrow-band nature of the tones observed, as well as their

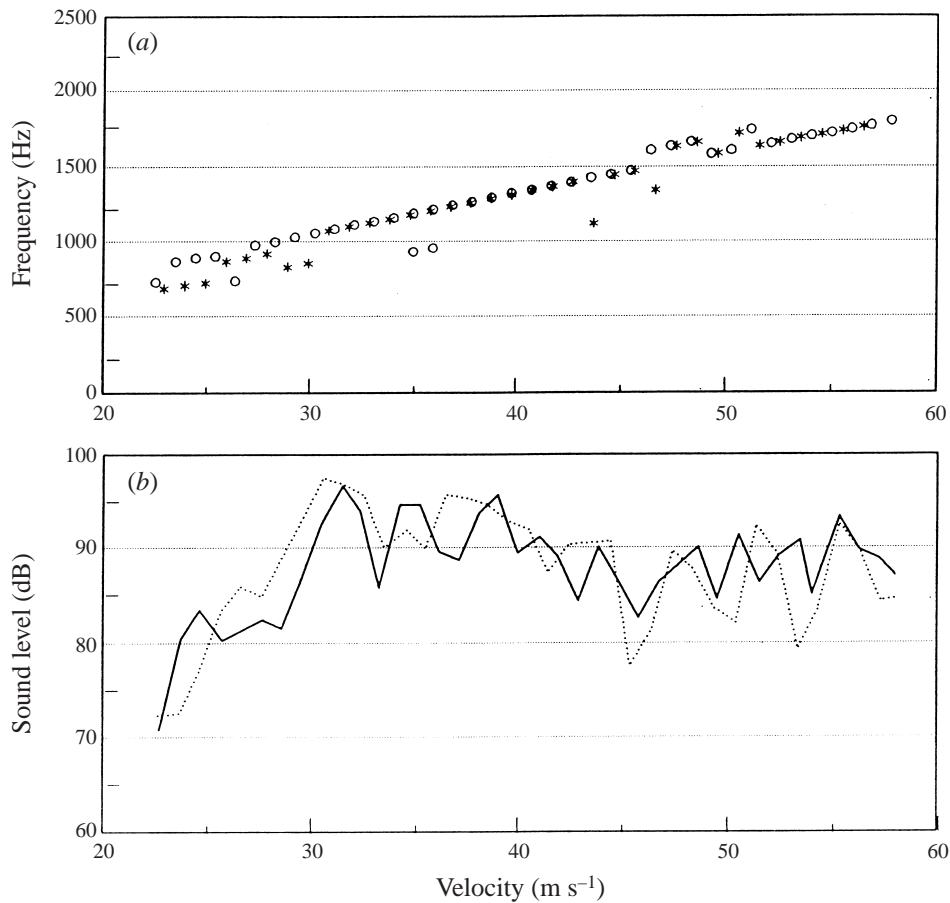


FIGURE 6. Repeatability of peak frequencies quasi-anechoic tunnel -4° . \circ and $—$, data set 1; $*$ and \dots , data set 2.

relation to wind-tunnel velocity, and the range of frequencies generated, confirms that the mechanism studied here was the same as that studied by previous researchers.

It is believed that previous investigators may have been misled by spurious feedback loops which have arisen from the particular features of the rig, even in open-jet studies. The present experiments show that the frequency structure in a more carefully controlled environment has little sign of these feedback processes. This is believed to be more representative of the practical situation. This set-up was employed for the remainder of the results reported.

Figure 6(a) and 6(b) show the repeatability of the measured frequencies and sound levels for -4° angle of incidence. It can be seen that the two cases shown in figure 6(a), which were taken several months apart, show close agreement of measured frequencies, with some scatter at lower velocities and around 50 m s^{-1} . This allowed repeatable measurements to be made over a long period of time. The measured sound levels showed less repeatability, as shown in figure 6(b). This was despite careful calibration of the microphone at the beginning of each day of testing. Discrepancies of up to 5 dB were observed over the measured range of frequencies. Measured sound levels are seen to rise initially, then flatten out with increased wind-tunnel velocity, although the data fluctuates too much to observe a simple relationship between

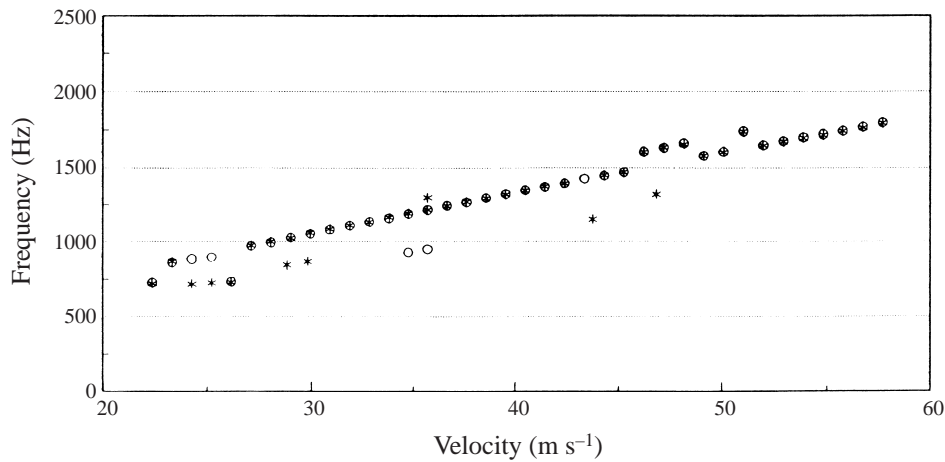


FIGURE 7. Comparison of peak frequencies at -4° with tunnel velocity \circ , increasing and $*$, decreasing.

sound level and wind-tunnel velocity. A comparison of frequencies measured with the wind-tunnel velocity increasing and decreasing (figure 7) showed that there was no hysteresis effect of wind-tunnel velocity.

4. Spectral measurements using the LDA

4.1. Basic measurement technique

Initial measurements were undertaken using both hot-wire and LDA techniques. As reported in Nash & Lowson (1995) it was found that the hot-wire support caused significant interference with the flow. It became clear that hot-wire measurements could not be relied upon in the separated region of interest. Thus, it was necessary to undertake the measurements using an LDA, taking advantage of techniques developed within the group and reported by Barrett & Swales (1998).

Performing spectral analysis with LDAs requires high-quality data with a sufficient data rate and high signal-to-noise ratio. Complex data processing is required to obtain spectral information from the intermittently collected data. In general it has been found that a data rate of about 10 times the maximum frequency of interest is necessary, e.g. Djenidi & Antonia (1995). Factors that must be considered in order to achieve the maximum possible data rate are discussed in detail by Swales (1994). The two most significant influences on data rate for measurements presented here were the quality of alignment and the density of seeding.

In order to determine the frequency content of the flow non-intrusively, the scattered light received by the collecting optic head of the LDA was connected to a Dantec analogue tracker (Type 55N21) which was used in conjunction with a Dantec frequency shifter (Type 55N11). This enabled the analogue signal output from the tracker to be connected directly to a Brüel and Kjær (B & K) frequency analyser for spectral analysis. The additional seeding necessary when using the analogue tracker to obtain a high enough data rate was produced using a water-based fogger. This enabled free-stream data rates of over 40 kHz to be obtained, over a limited time period.

A number of further improvements were made to the equipment. An investigation was also made into the effect of data rate and BSA settings on the BSA analogue

output, and values chosen which provided a satisfactory measurement process. These are discussed in detail in Nash (1996).

The LDA was used to simultaneously measure three components of velocity, i.e. the streamwise, spanwise and vertical components of the flow near the trailing edge of the NACA0012 aerofoil for selected test cases. The procedure employed for three-dimensional alignment is described in Swales *et al.* (1993), and has proved to be extremely successful, and critical to the achievement of the present results.

4.2. LDA results

Results from eight separate cases are presented in Nash (1996). In the present paper, only two cases will be discussed in detail, corresponding to conditions with and without tones. Case 1, with the tone present, is for a velocity of 29.7 m s^{-1} at an incidence of -4° , and produces a frequency of 1048 Hz. Case 2, with no acoustic tone, is for a velocity of 8.1 m s^{-1} at an incidence of -3° . For all data presented, the given distance from the trailing edge refers to the distance upstream of the trailing edge unless otherwise specified. All mean and r.m.s. velocity fluctuation profiles presented are for streamwise velocities unless otherwise specified.

Mean and r.m.s. velocity fluctuation boundary-layer profiles are shown in figure 8 for case 1. At 35 and 25 mm from the trailing edge, the flow is attached and laminar, which is confirmed by the corresponding r.m.s. velocity fluctuation profiles which exhibit one peak at half boundary-layer thickness. The second r.m.s. velocity fluctuation peak predicted to occur at the top of the boundary layer is below background turbulence levels. At 20 mm, the boundary layer is at the point of separation, and a small secondary r.m.s. velocity fluctuation peak occurs at the aerofoil surface. All mean velocity profiles downstream from this point show separated flow. The mean velocity profile at 5 mm from the trailing edge passes from a region of reversed flow back to flow in the streamwise direction before approaching zero near the surface. The r.m.s. velocity fluctuation profiles for the separated flow show the triple-peaked distribution throughout the boundary layer, which is due to amplified boundary-layer instabilities, as discussed by Nash & Lowson (1995). A remarkable feature of the triple-peaked r.m.s. velocity fluctuation profiles is that the r.m.s. velocity fluctuation does not reach a steady value until approximately twice the boundary-layer thickness (based on 99 % free-stream velocity). Another notable characteristic is the considerable unsteadiness of the boundary layer, which attains an r.m.s. velocity fluctuation of 7.5 m s^{-1} at the trailing edge. Figure 9(a) and 9(b) show three sets of data taken consecutively for mean and r.m.s. velocity fluctuation profiles 5 mm from the trailing edge for case 1. This figure demonstrates that the characteristics of the boundary layer, particularly the r.m.s. profile, are a repeatable feature of this flow.

Figure 10 shows u , v and w r.m.s. velocity fluctuation profiles measured 5 mm from the trailing edge for case 1. The u component shows the typical triple peaked r.m.s. distribution. All three r.m.s. velocity fluctuation components show a local minimum at 1 mm from the surface. The vertical, or w , r.m.s. velocity fluctuation reaches a maximum within the boundary layer but is lower than for the u r.m.s. velocity fluctuation component. These results are in excellent agreement with theoretically calculated streamwise and vertical amplitudes of disturbance presented in Dovgal, Kozlov & Michalke (1994). The spanwise, v , r.m.s. velocity fluctuation component is much lower, although a peak v r.m.s. velocity fluctuation content is apparent within the boundary layer. This indicates that there is a degree of spanwise flow, or three-dimensionality, within the separated region.

Figures 11(a)–11(f) show velocity histograms for case 1, extending beyond the

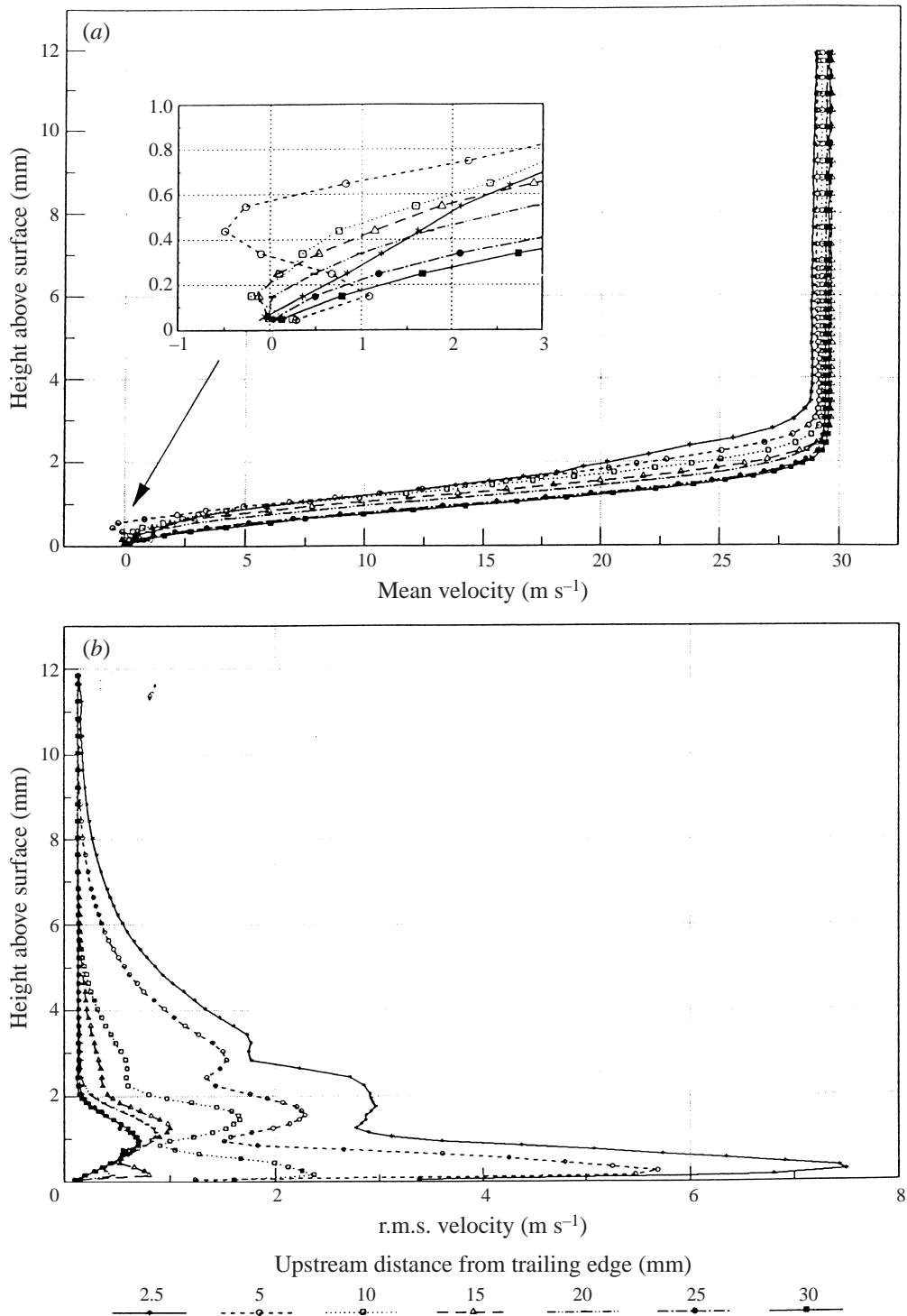


FIGURE 8. (a) Mean and (b) r.m.s. velocity fluctuation boundary layer profiles for case 1.

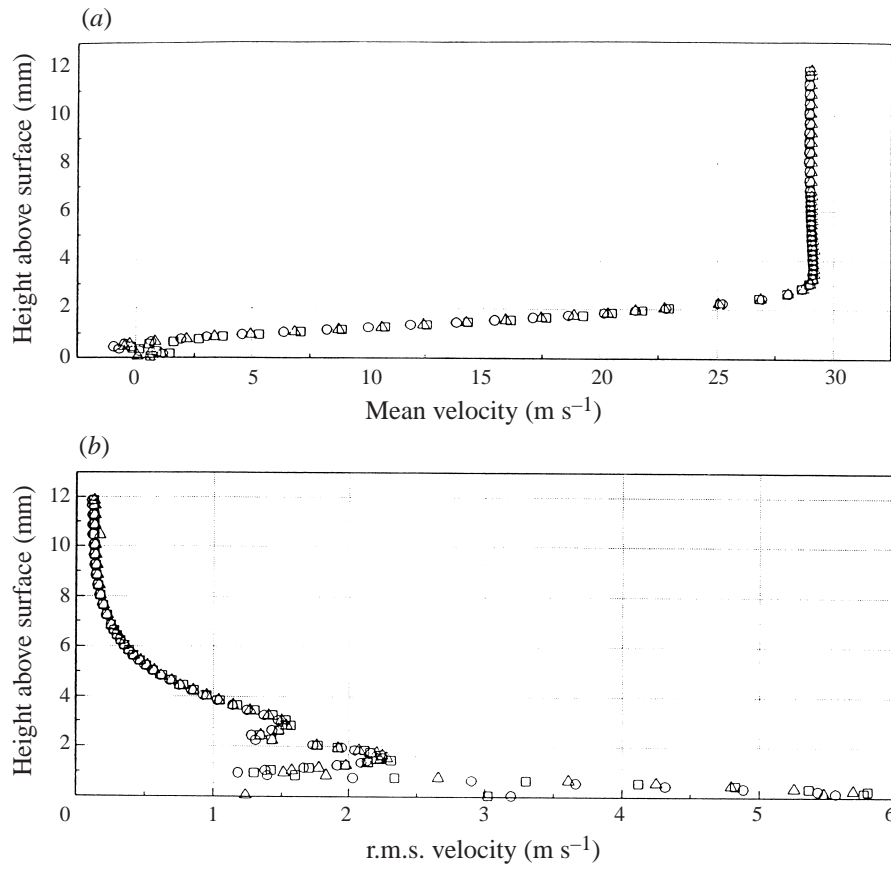


FIGURE 9. A comparison of three (a) mean and (b) r.m.s. velocity fluctuation profiles measured 5 mm upstream from the trailing edge for case 1. \square , test 1; \triangle , test 2; \circ , test 3.

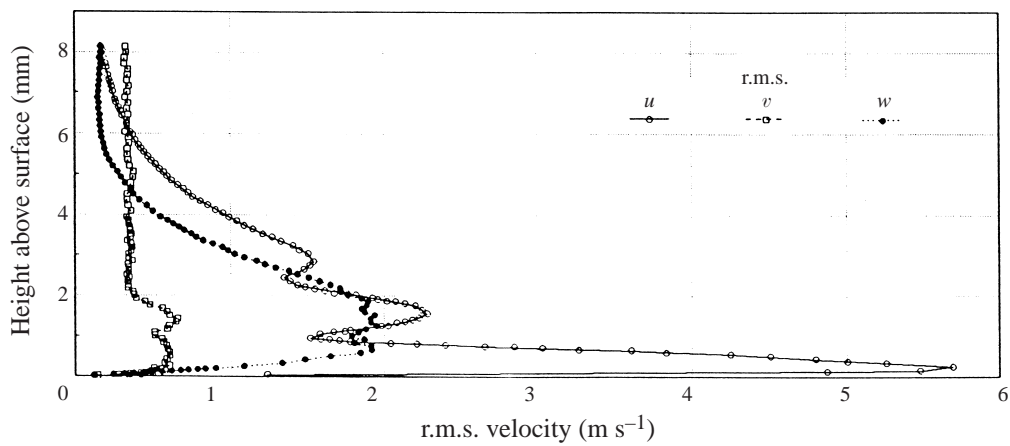


FIGURE 10. u , v and w r.m.s. velocity fluctuation profiles measured 5 mm upstream from the trailing edge for case 1.

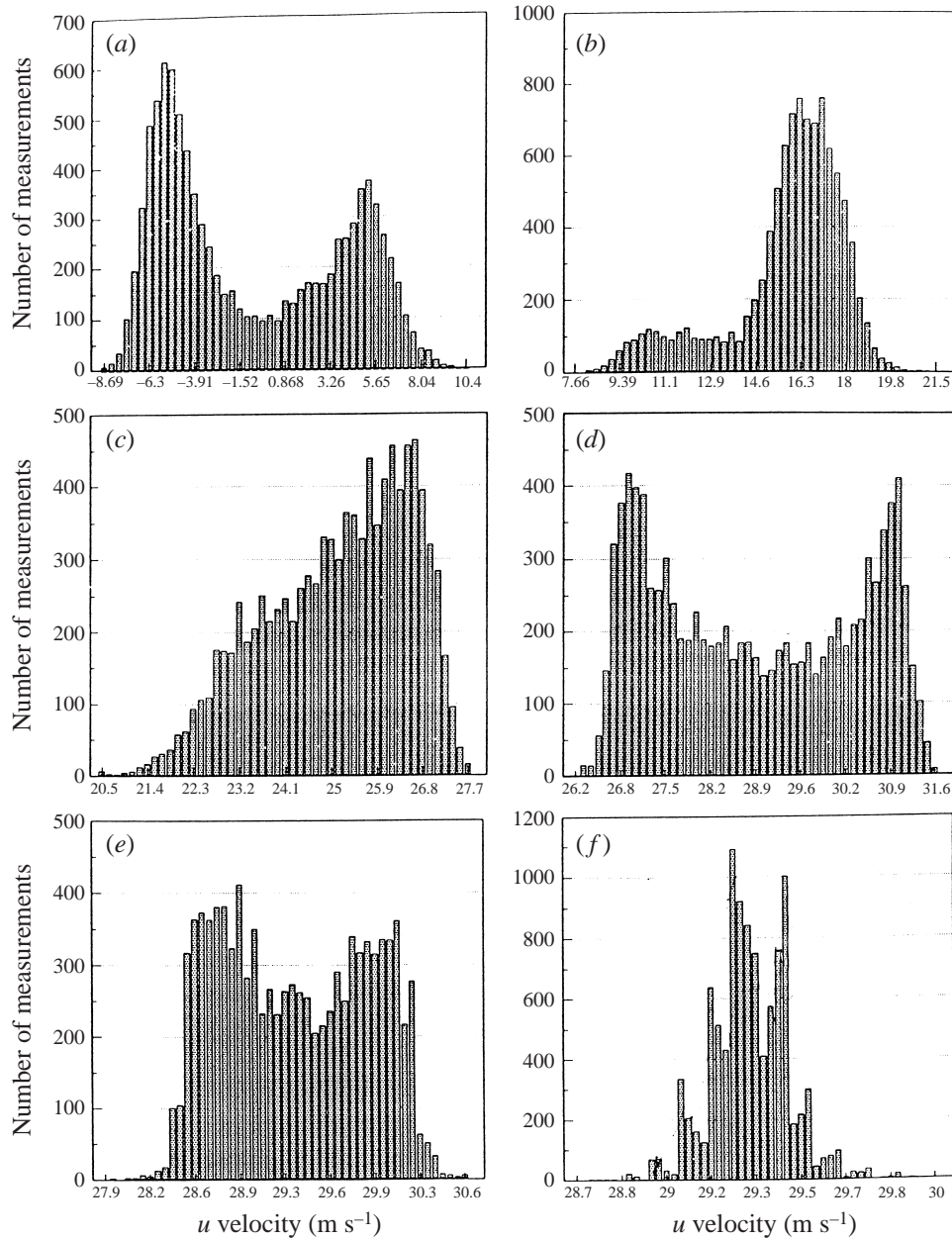


FIGURE 11. LDA velocity histograms for case 1, 5 mm from the trailing edge. Distance from the surface: (a) 0.4 mm; (b) 1.55 mm; (c) 2.25 mm; (d) 2.84 mm; (e) 5 mm; (f) 11.85 mm.

boundary layer up to 11.85 mm from the surface. At 0.4 mm from the surface, within the reversed flow region, there is a large-scale fluctuation of about $\pm 6 \text{ m s}^{-1}$ in a mean flow of -0.05 m s^{-1} which leads to a sinusoidal shaped velocity distribution. Figure 10 shows there are two further r.m.s. velocity fluctuation peaks above the separated flow, one at half the thickness of the shear layer, 1.55 mm from the surface, and another at the top of the boundary layer, 2.84 mm from the surface. Velocity histograms are presented to correspond to these peaks. At 1.55 mm and 2.25 mm the histograms are

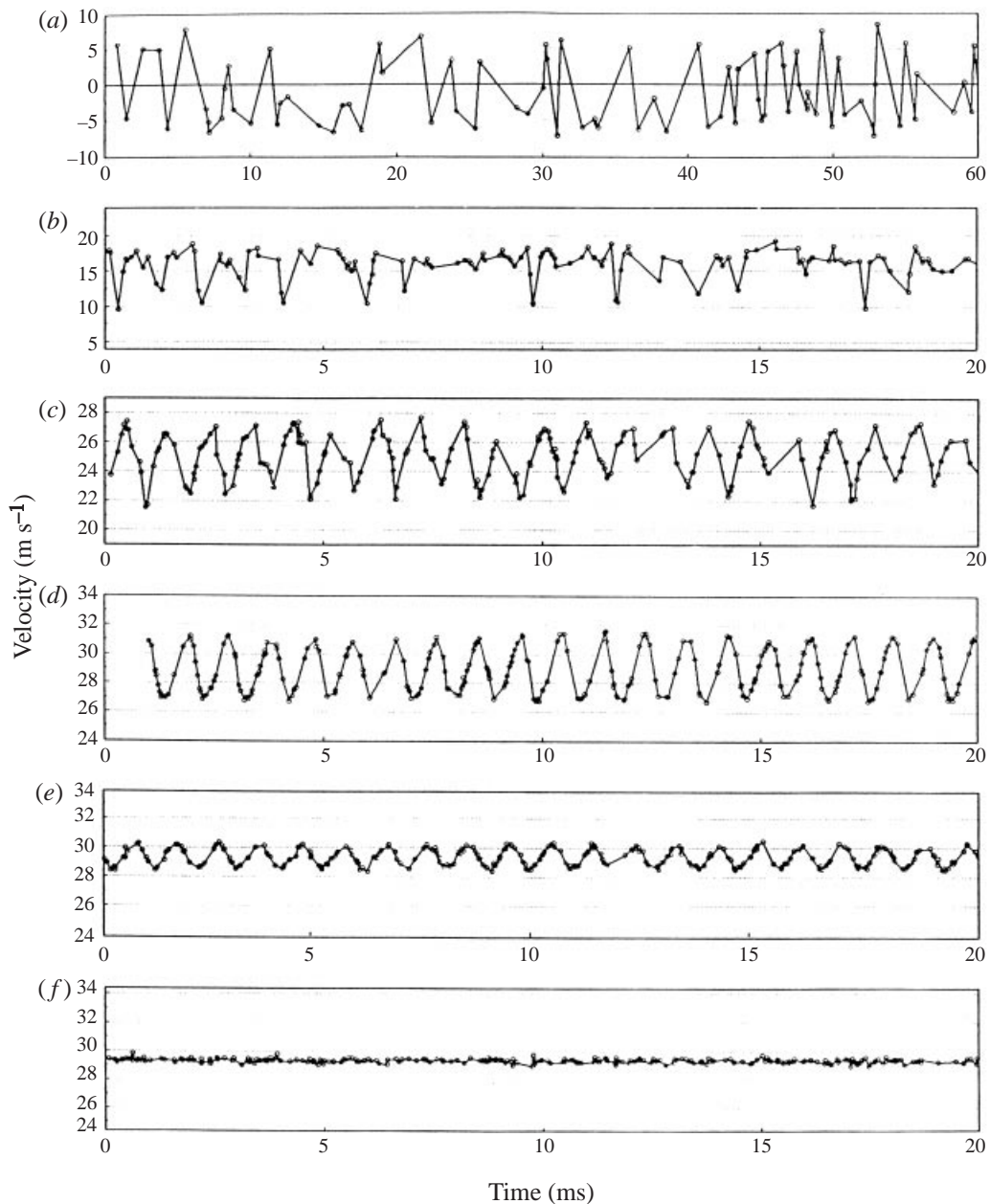


FIGURE 12. LDA time series for case 1, 5 mm upstream from the trailing edge. Distance from the surface, data rate: (a) 0.4 mm, 1.4 kHz; (b) 1.55 mm, 7.21 kHz; (c) 2.25 mm, 9.81 kHz; (d) 2.84 mm, 14 kHz; (e) 5 mm, 14.21 kHz; (f) 11.85 mm, 14.22 kHz.

highly asymmetrical. The sinusoidal distribution returns at 2.84 mm and is maintained up to 5 mm from the surface, even though this is well out of the boundary layer. At 11.85 mm from the surface, the velocity histogram would be expected to show a Gaussian distribution, but is instead shown to be highly irregular in shape.

The unsteady flows are characterized by a highly ordered periodic structure in the main body of the flow. This is demonstrated in the time-series plots of figure 12. The

alternating flow between $\pm 6 \text{ m s}^{-1}$ at 0.4 mm is clearly demonstrated. This indicates a large-scale ‘flapping’ which is consistent with the features of unsteady separated flow. At 1.55 mm from the surface, the time series is characterized by less frequent, but substantial, velocity spikes at 10 m s^{-1} (note the change in scale of the y -axis between 1.55 and 2.25 mm). A possible explanation for this effect would be that it was due to a flapping motion of the whole separation bubble, which only occasionally reaches the lower levels. However, the asymmetrical velocity histogram at this height (figure 11 *b*) exhibits a velocity ‘tail’ which often indicates the presence of vortical flow. The shear layer is an area of high local spanwise vorticity which can be expected to roll up into a concentrated form. It is therefore likely that the results shown derive from some convected vortical structure. The periodic velocity fluctuations shown in the time series of figure 12 (*c*) show a saw-toothed waveform, and again correspond to a asymmetric velocity histogram. At 2.84 mm and 5 mm from the surface (figure 12 *d* and 12 *e*), the time series have become almost sinusoidal and correspond to the sinusoidal-shaped velocity histograms. There appears to be no periodic structure to the time series of figure 12 (*f*). Digital spectral data taken for this case are consistent with the observed signal time histories and show the same single peak frequency over the whole of the boundary layer, with a magnitude dependent on location.

The mean velocity profiles for case 2, in which no tone is present, shown in figure 13, show a substantial region of reversed flow extending from 55 mm from the trailing edge up to the trailing edge. However, the corresponding r.m.s. velocity fluctuation profiles are significantly different to those measured in the presence of an acoustic tone. First, the r.m.s. velocity fluctuation values are notably lower than for the previous cases presented, with a maximum value of less than 0.3 m s^{-1} . Secondly, at all stations measured, the r.m.s. velocity fluctuation profiles display, at most, two peaks rather than the expected triple-peaked profiles. A reason for the low r.m.s. velocity fluctuation values is provided by the time series and velocity histograms in figure 14 (*a*) and 14 (*b*). There is no evidence of a highly amplified periodic content to the time series at any point in the boundary layers at 35 mm and 0.5 mm from the trailing edge and the velocity histograms display a Gaussian distribution. Corresponding frequency-spectra measurements show no peak frequency at either chordwise station. There is clearly no selectively amplified instability within this flow, and as a direct result of this, there is no acoustic tone. A physical explanation for the absence of any periodicity in the flow is less obvious and warrants further work, although a possible reason is provided in §7.

The results show that separation alone is not enough to generate a tone. There must be an extended region of inflection to allow the amplification of boundary-layer instabilities. The generation of an acoustic tone is intrinsically linked to the presence of a large-scale periodic content at the aerofoil trailing edge. These fluctuations are believed to be due to T–S waves which are highly amplified in the separated free shear layer near the trailing edge. These conditions for tone generation are summarized as:

- (i) There must be a region of separated, or inflected flow near the aerofoil trailing edge in order to provide an amplification mechanism for T–S instabilities.
- (ii) The separated or inflected flow must be close enough to the trailing edge to maintain a periodic structure to the trailing edge.
- (iii) The adverse pressure gradient at the trailing edge must not be too great so as to initiate non-coherent, random turbulence.

At high enough velocities the tones disappear since the flow has become turbulent owing to natural transition upstream of an inflectional or separated boundary layer, thereby preventing the strong amplification of T–S boundary-layer instabilities.

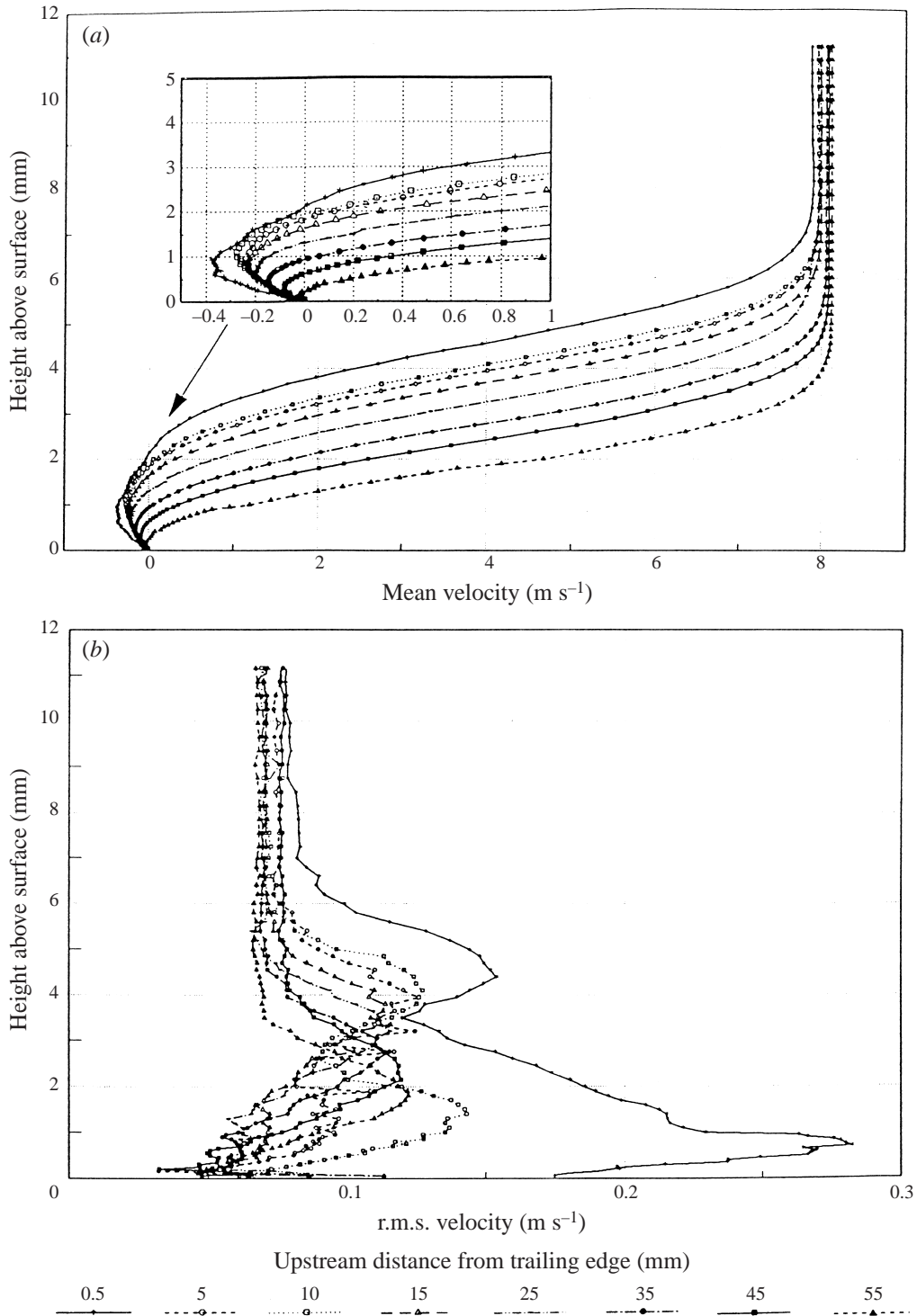


FIGURE 13. (a) Mean and (b) r.m.s. velocity fluctuation profiles for case 2.

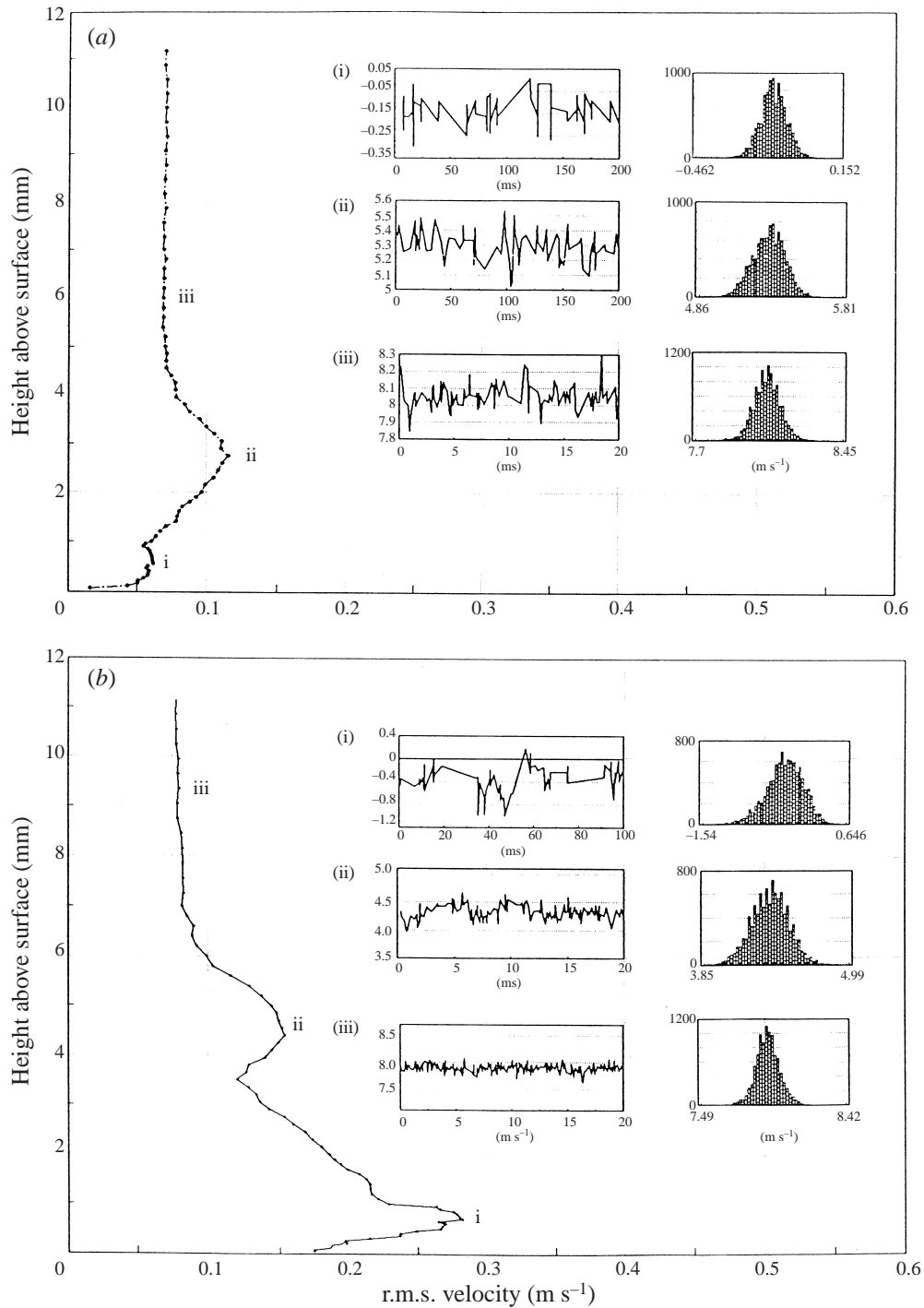


FIGURE 14. (a) Time series and histograms for case 2, 35 mm upstream from the trailing edge. (b) Time series and histograms for case 2, 0.5 mm upstream from the trailing edge.

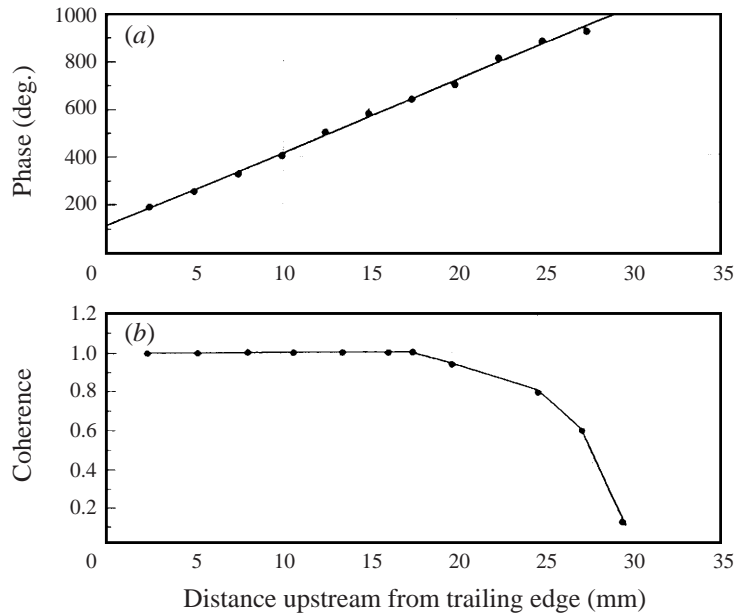


FIGURE 15. Phase and coherence between tracker and microphone 3 mm from surface for case 1. Averaged wavelength = 11.4 mm; $u/U = 0.4$.

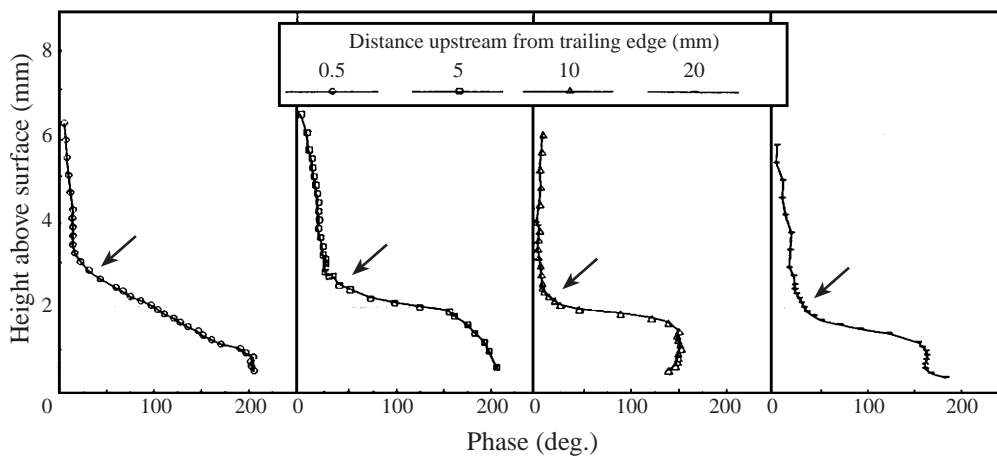


FIGURE 16. Change in phase through boundary layer between BSA analogue output and microphone, Case 1. Arrowhead indicates top of the boundary layer.

4.3. Analogue spectral and cross-spectral measurements

Figures 15 and 16 are taken from case 1 and show the chordwise change in phase of the boundary-layer instability at 3 mm above the surface. It can be deduced from this that the wavelength of the instability is 11.4 mm and travels with a phase velocity of 40% U . Figure 15(b) shows that the coherence between the microphone and tracker at 3 mm above the surface is a maximum of 1.0 until 17.5 mm from the trailing edge. Coherence falls to 0.1 at 30 mm from the trailing edge, which is upstream of the point of separation. This coherence data correlates well with the frequency spectra which show a substantial peak frequency up to 15 mm from the trailing edge, which

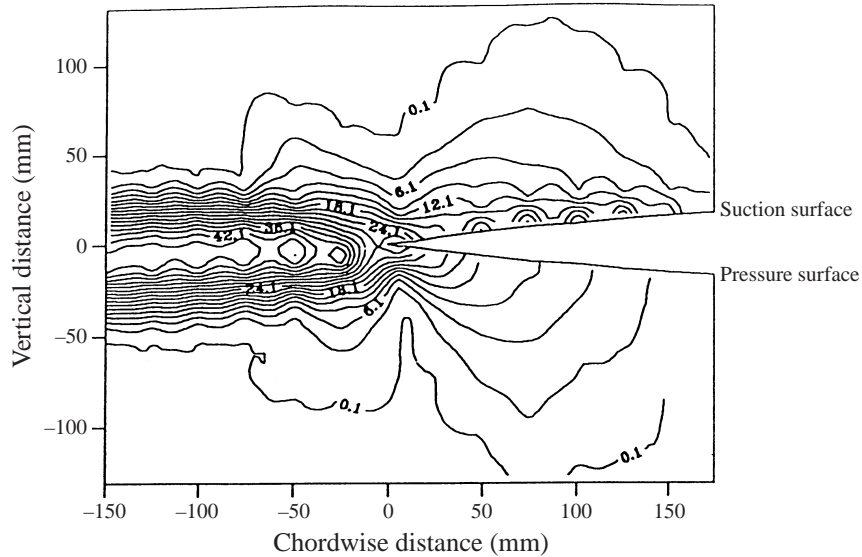


FIGURE 17. u perturbation contours in the mean flow at 1048 Hz for case 1.

then drops to a level too small to be detected above background noise at 30 mm from the trailing edge. This coherence data confirms that the discrete frequency noise generation is directly related to the region of trailing-edge separated flow.

Figure 16 shows a series of boundary-layer phase profiles taken for case 1 with the BSA analogue output referenced to the microphone. It can be seen that, for all four profiles shown, there is a change in phase at the top of the boundary layer. Measurements taken with the LDA showed the phase shift to occur as a single and continuous 180° shift at 0.5 and 5 mm from the trailing edge. At 10 and 20 mm from the trailing edge, the phase shift occurred as a 130° shift at the top of the boundary layer with a second phase shift near the surface. These results show a fair agreement with those of Gaster (1966) although they were taken non-intrusively whereas hot-wire probe disturbance may have been present during Gaster's experiments, leading to the slight discrepancy with the results presented here. All the phase data in figure 16 were taken with a constant data rate of 3 kHz, which did not allow data to be taken closer than 0.5 mm from the surface.

4.4. Peak velocity perturbation amplitude profiles

Figure 17 presents contour plots of the streamwise peak amplitude of oscillation. Measurements were taken with a data rate of 25 kHz. The values on the contours are in decibels and show the peak value above background turbulence. The contour plots show that no peak-frequency component within the flow was observed above background turbulence upstream of 50% chord on the pressure surface and 58% chord on the suction surface. However, downstream of these chordwise stations, an extensive region of free-stream flow disturbance was detected which extended up to 110 mm from the surface and into the wake. On the suction surface of the aerofoil, the peak-frequency value was swamped by high background noise at 5 mm from the surface owing to the presence of a thick, highly turbulent boundary layer. The wavelike pattern on the suction surface of figures 17 and 18 is a result of the contour plot interpolation process, and has no relevance to the flow behaviour at the surface.

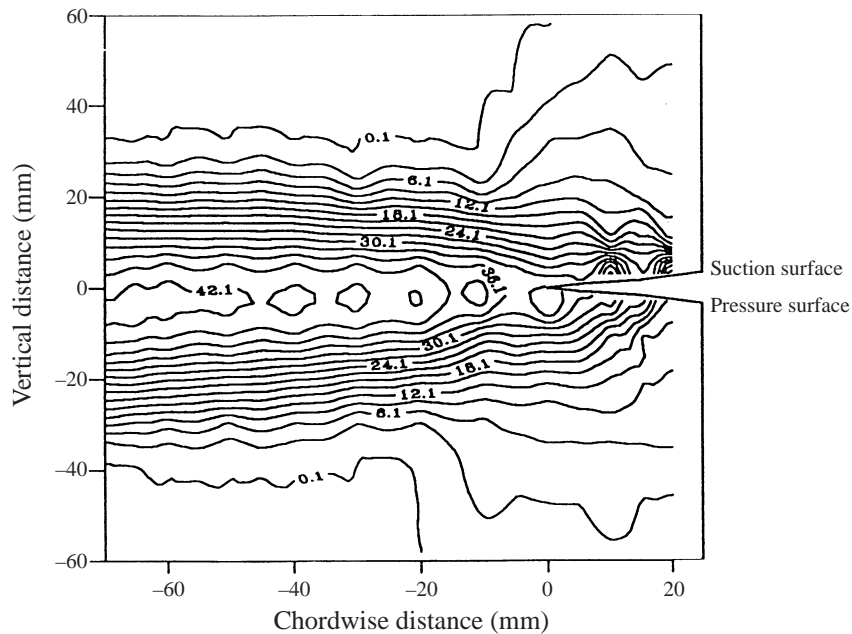


FIGURE 18. w perturbation contours in the mean flow at 1048 Hz for case 1.

It is well documented that eddies passing over a sharp aerofoil trailing edge will generate a large-scale acoustic field in the mean flow (Ffowcs Williams & Hall 1970). The diffraction of a T-S wave at the end of a flat plate in a uniform flow, namely the Blasius boundary layer, was considered by Aizin (1992). He examined the problem of a T-S wave incident on the edge of the plate in the near-field, assuming incompressibility. The solution was compared to the wave equation in the far field to obtain an analytic expression for the resulting acoustic radiation. The frequency of the sound was the same as that of the T-S wave. Our experimental results confirm that scattering of an instability at the edge of the plate generates an oscillating hydrodynamic and acoustic field at the same frequency as the instability of the boundary layer. Figure 17 shows there is an oscillating hydrodynamic field about the trailing edge of the aerofoil, with the same frequency as the T-S wave in the boundary layer.

It has been established for many years that the strength and narrow-band nature of the acoustic tones, as well as the observed ladder-like structure of tones with increased velocity, requires a feedback mechanism for the generation process. This feedback mechanism has remained unclarified but was believed to be acoustic in nature. However, the large-scale hydrodynamic oscillating field shown to exist here is likely to play a major role in the feedback-loop process of the tonal noise-generation mechanism by providing direct excitation of the boundary layer.

A corresponding plot of vertical free-stream flow oscillations is presented in figure 18. It can be seen that the region of vertical free-stream flow oscillations is far less extensive than for the streamwise oscillations, and does not reach as far upstream from the trailing edge or into the wake. However, the magnitude of vertical oscillations matches those of the streamwise oscillations near the trailing edge. The extent of the vertical flow oscillations at the trailing edge provides important information on the applicability of the Kutta condition at the trailing edge to the unsteady flow observed. The acoustic modelling of aerofoil noise is extremely sensitive to the trailing-edge conditions assumed. However, the experimental evidence on the validity

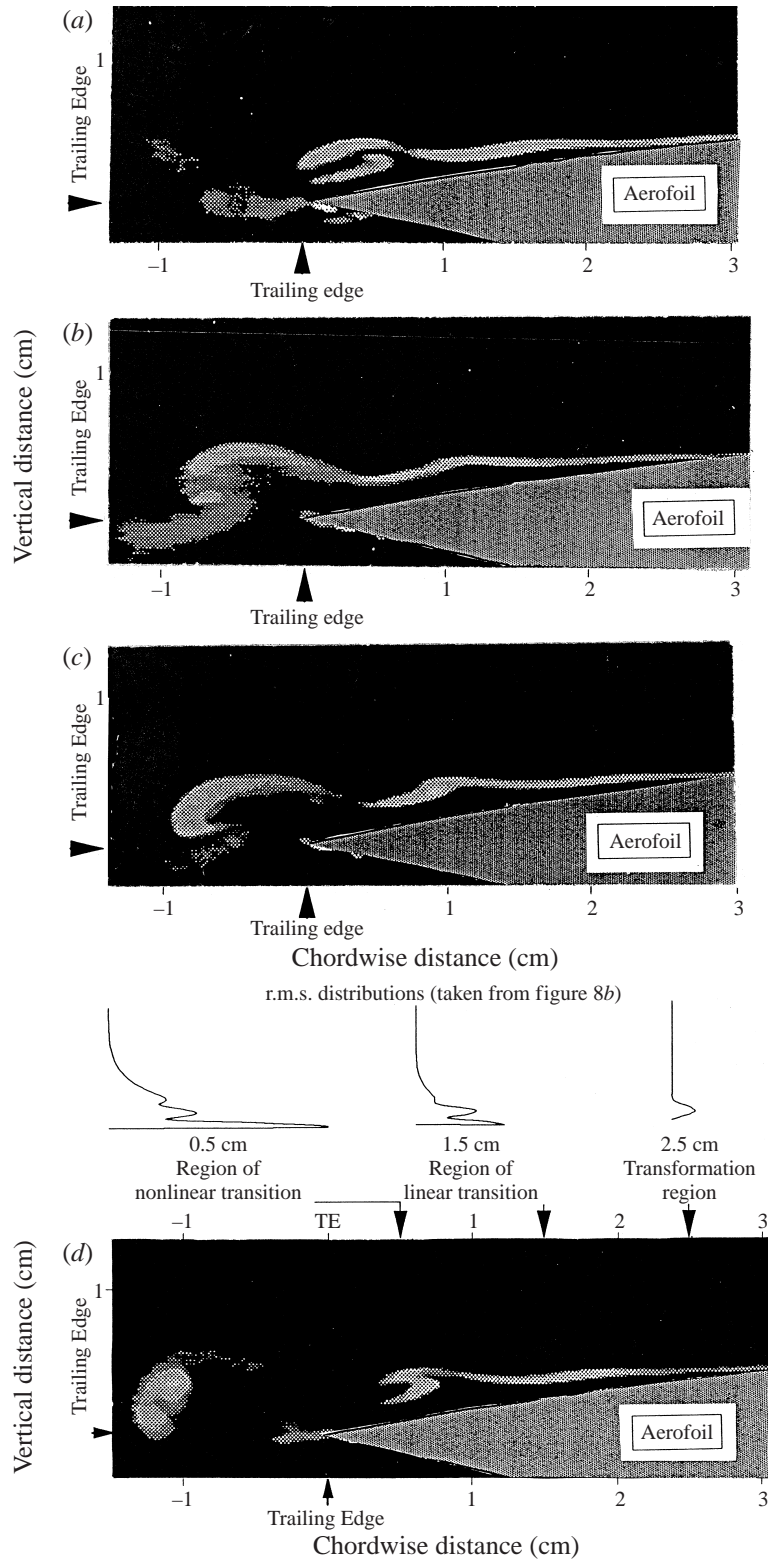


FIGURE 19. For caption see facing page.

range of the Kutta condition is mixed. The usual theoretical assumption is that no pressure difference can be sustained across the aerofoil trailing edge, and in this model the streamlines adjacent to the aerofoil leave tangentially to either the upper or lower surface. Furthermore, the wake is assumed to remain thin and straight, or at least follow a steady flow streamline. Figure 18 shows that the magnitude of the flow oscillations in the vertical direction does not tend to zero at the trailing edge, which is a violation of the unsteady Kutta condition.

Previous flow visualization experiments have shown that an aerofoil wake has a strong tendency to organize itself into a series of vortices, particularly in the presence of trailing-edge separation for which the Kutta condition can no longer be applied. Archibald (1975*b*) reports that the most severe violation of the Kutta condition occurs in the case of acoustically correlated vortex shedding. Smoke streakline flow visualization was carried out to observe the behaviour of the flow over the trailing edge and into the wake for case 1. These experiments and results are described in detail in § 5. They show a periodic vortex street to be shed at the frequency of the acoustic tone generated. Thus the present results are consistent with those of Archibald (1975*b*).

5. Flow visualization

The LDA yielded some important results throughout the investigation, but it was still unclear exactly how the flow behaved as it passed over the trailing edge and into the wake using. Therefore, smoke streakline flow visualization was performed to observe the flow structure at the aerofoil trailing edge and into the wake using titanium tetrachloride (Freymuth 1989). A few drops of TiCl_4 were introduced by pipette onto the surface of the aerofoil at approximately 70% chord, which was upstream of separation, but close enough to maintain a dense filament of smoke over the trailing edge. By introducing the smoke onto the surface of the aerofoil, the problem of observing 'false' vortex cores, as pointed out by Hama (1962), is avoided. When titanium oxide deposits began to develop on the aerofoil, the test was stopped, and the surface cleaned.

The tests were recorded on a Hi-8 video camera through the test-section window. The tunnel velocity was 29.7 m s^{-1} and the acoustic tone was 1048 Hz, as for case 1. A laser light sheet was used to illuminate the flow, using either an oscillating mirror or a cylindrical rod to generate the laser light sheet. Use of the oscillating mirror allowed the light to be strobed to the flow, allowing the unsteadiness to be observed by eye. Alternatively, the laser beam was passed through a rotating 60 slit strobe disk before passing through the cylindrical lens. This successfully froze the observed flow which was recorded on a Hi-8 video at 120 frames per second. Still images were recovered from the video by a frame-grabber.

Figure 19 shows digitally recovered images from the Hi-8 video film taken of the TiCl_4 flow visualization experiments for case 1 using the rotating mirror. It should be noted that the images shown here did not follow sequentially in time, but have been selected to best demonstrate the flow characteristics that were observed. Figure 19 (*a*) shows the formation of a vortex at the aerofoil trailing edge. As the vortex is shed from the trailing edge, another highly amplified instability wave forms at 10 mm

FIGURE 19. Smoke visualization at the pressure surface trailing edge for case 1. (*a*) Instability begins to roll up near the trailing edge. (*b*) Instability rolls up into a vortex at the trailing edge and a second instability begins to form. (*c*) Second instability begins to roll up. (*d*) A vortex is shed from the trailing edge, as the second instability rolls up into a vortex.

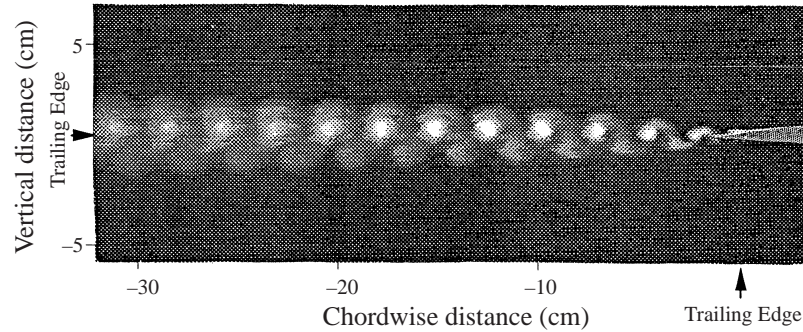


FIGURE 20. Smoke flow visualization of the wake for case 1.

from the trailing edge (figure 19 *b, c*). This instability wave rolls up to form a second vortex, shown in figure 19 (*d*), as the first vortex is shed into the wake. On comparing these flow-visualization pictures with the r.m.s. boundary-layer profiles of case 1, similar conclusions are found to those of Freymuth (1989). Freymuth investigated the growth of small disturbances in an excited jet by hot-wire measurements and flow visualization. Four regions of transition were identified by Freymuth, three of which can be detected here, as illustrated in figure 19 (*d*). The first of these is where only one r.m.s. maximum exists and a transformation process takes place so that in the following region exponential growth is possible. For the case visualized here, this region is at the beginning of free shear flow at 25 mm from the trailing edge. Further downstream, the disturbances grow exponentially and the r.m.s. distribution contains two maxima. This region of linear transition is followed by the third region, 5 mm from the trailing edge, called the nonlinear region. This is characterized by vortices, where three maxima in the r.m.s. distribution occur which later coalesce to form two. Such coalesced r.m.s. maxima were found in the high-speed cases examined. Freymuth names a fourth region, which is turbulence where only one r.m.s. peak occurs. This is shown to be the case at the trailing edge for the no-tone case.

The resulting wake pattern in figure 20, obtained using the strobe disk, shows that a regular vortex street is shed from the trailing edge. A row of vortices are observed to be shed from the pressure (upper) surface which are shed alternately with a second row of vortices entrained into the smoke from the lower surface. This observed vortex shedding is of the form of a von Kármán vortex street where the ratio of the vertical to horizontal spacing of the vortices is 0.3 which is close to 0.281, the value theoretically obtained by von Kármán.

It can be reasoned that the observed vortices are shed at the same frequency as the acoustic tone because the flow was 'frozen' by the strobe at 1048 Hz. The highly regular structure of the vortex street accounts for the pure narrow-band acoustic tone that is observed. These findings provide additional evidence that the generation of acoustic tones is dependent on the presence of a region of separated flow just upstream of the trailing edge of the laminar flow surface, in this case the pressure surface.

6. Theoretical modelling of instability characteristics

6.1. Introduction

Previous theoretical attempts to predict the frequency of acoustic tones generated by an aerofoil used either stability characteristics calculated for flow over a flat plate

Station	Chord (%)	Station	Chord (%)
1	0.2800	7	0.75
2	0.3333	8	0.833
3	0.4166	9	0.8833
4	0.5	10	0.9166
5	0.5833	11	0.9333
6	0.6666	12	0.9666

TABLE 1. Chordwise locations of stations used for theoretical predictions.

assuming zero pressure gradient (Tam 1974; Fink *et al.* 1976; Longhouse 1977; Fink 1978; Arbey & Bataille 1983) or, selected one Hartree profile as an attempt to model the adverse pressure gradient beyond midchord on an aerofoil (Archibald 1975a). This approach does not take into account the effect of significant pressure gradient changes around the aerofoil and, importantly, the effect of trailing-edge separation on instability behaviour cannot be modelled. The aim of the work described in this section was to understand more closely the role of boundary-layer instabilities in generating tonal noise, particularly in the presence of separated flow. The generation of boundary-layer instabilities over most of the aerofoil pressure surface was studied, rather than just at the trailing edge as previously considered by the workers listed above. For a detailed summary of the theoretical investigation of boundary-layer instabilities generating tonal noise see McAlpine (1997) and McAlpine, Nash & Lawson (1999).

6.2. The modelling of instability

A technique to model the instability behaviour theoretically over the NACA0012 aerofoil was employed for cases 1 and 2. The Falkner–Skan (F–S) boundary layer was used to model the flow at a series of chordwise stations along the aerofoil because it can represent boundary layers with adverse pressure gradients. The F–S equation provides a series of similar solutions, known as Hartree profiles, for different wedges of semi-angle $\frac{1}{2}\pi\beta_H$. For each value of $\frac{1}{2}\pi\beta_H$ there is a unique value of the shape factor, H , for the boundary layer along the wedge. The boundary layer was defined at twelve stations across the chord. These are listed in table 1. Profiles close to separation were typically at about 80% chord between stations 7 and 8. At each station the shape factor was defined from a combination of measurement and prediction, and the flow at the station was modelled by an F–S boundary layer with the same shape factor. Also, the pressure gradients around the aerofoil were predicted theoretically using the method of Soinnie & Laine (1988). It was found that by matching the shape factors at each chordwise station, the pressure gradient calculated from the selected F–S profile matched that calculated for the aerofoil typically to within 20%. Then the Orr–Sommerfeld (O–S) equation was solved at each station on the aerofoil by using the F–S velocity profiles. The free-stream velocity U and the boundary-layer displacement thickness δ^* were taken to be the characteristic velocity and lengthscales respectively. At each station, the Reynolds number $R_{\delta^*} = U\delta^*/\nu$ was fixed for each case. By choosing a frequency f (which translates to a non-dimensional frequency $\varpi = 2\pi f\delta^*/U$), the solution of the O–S equation gives the complex wavenumber, $\alpha = \alpha_r + i\alpha_i$, where α_r is the wavenumber and $-\alpha_i$ the growth rate at each station. Thus, a picture of boundary-layer instability over the whole adverse pressure surface was assembled.

In this approach, the contribution of traditional T–S waves in the attached part of the boundary layer, and from inviscid Rayleigh waves arising from inflectional profiles, are combined, so that no distinction between these forms of instability occurs. However, it is clear that in the early parts of the boundary layer where the flow is attached the estimates are for instabilities which are essentially of T–S type, whereas in the separated shear layer the estimates refer to Rayleigh inflectional instabilities.

In order to use the O–S equation, several assumptions must be made regarding the flow under investigation. First, the flow is assumed to be laminar and quasi-parallel. It is assumed to be quasi-parallel if the boundary-layer thickness is approximately constant over one T–S instability wavelength. Secondly, the disturbances are assumed to be small and in the linear regime. Therefore, linear stability analysis was not conducted on the flow at stations past the point at which the flow was observed to become transitional, which was defined as the station at which the shape factor, H , began to decrease in value, indicating the onset of turbulent flow. For case 1, that transitional flow occurred at station 13. However, for case 2, the flow remained laminar to the trailing edge. Upstream of $x/c = 0.28$, the flow is not parallel and accelerates around the leading edge of the aerofoil, strongly damping any instabilities generated in this region (Dovgal & Kozlov 1983). Therefore, boundary-layer calculations were not carried out further upstream of this station for either aerofoil.

The method of obtaining the shape factor at each station around the aerofoil was determined according to its chordwise position along the pressure surface. For each case investigated, the separated-flow velocity profiles near the pressure surface trailing edge were measured with the laser-Doppler anemometer (LDA). The resulting mean velocity boundary-layer profiles were presented in figure 8(a) and were used to calculate the shape factors and displacement thicknesses, δ^* , required as the non-dimensionalizing lengthscale. Owing to time constraints, it was not possible to obtain experimental data over the entire pressure surface for each case investigated. Instead, a prediction program due to Fiddes was used to provide theoretical values of H and δ^* upstream of stations investigated with the LDA. This was only performed up to the theoretically predicted separation point. The theoretical separation point was always upstream of that measured experimentally.

To confirm that the prediction program was able to reliably predict values of H and δ^* , predicted values were compared with values of H and δ^* calculated from a number of boundary-layer profiles measured with the LDA at chordwise positions along the aerofoil pressure surface. This showed the r.m.s. error in prediction to be 3.1% for δ^* and 5.2% for H . It was concluded that this method of supplying H and δ^* upstream of experimentally measured stations was acceptable.

6.3. Results and discussion

Figure 21 shows neutral stability curves for the 12 stations along the NACA0012 aerofoil pressure surface for case 1. The stars represent the frequency of the observed acoustic tone against the Reynolds number at each station on the aerofoil. For station 3 onwards, the frequency lies within the unstable region of each curve. Figure 21 illustrates the enormous variation in instability behaviour of the flow over the aerofoil and confirms the inadequacy of using a single neutral instability curve to model such a flow. There is a particularly large change in the neutral instability curve structure between stations 7 and 8. This change in shape is reflected in the growth rate plots for the same case shown in figure 22, where the growth rates of the unstable frequencies increase dramatically between stations 7 and 8. The frequencies with the maximum growth rates close to the trailing edge are close to the observed

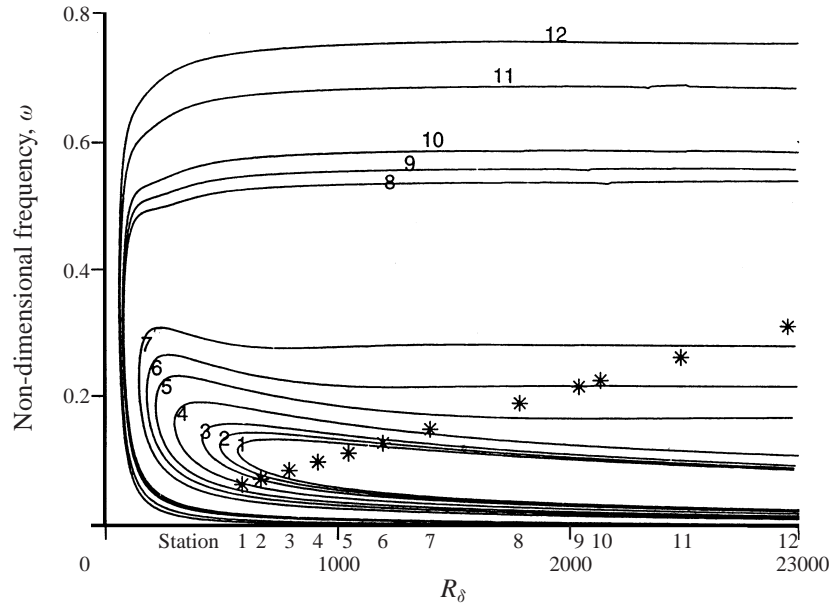


FIGURE 21. Neutral instability curve plots for stations 1 to 12 on the NACA0012 aerofoil for case 1.

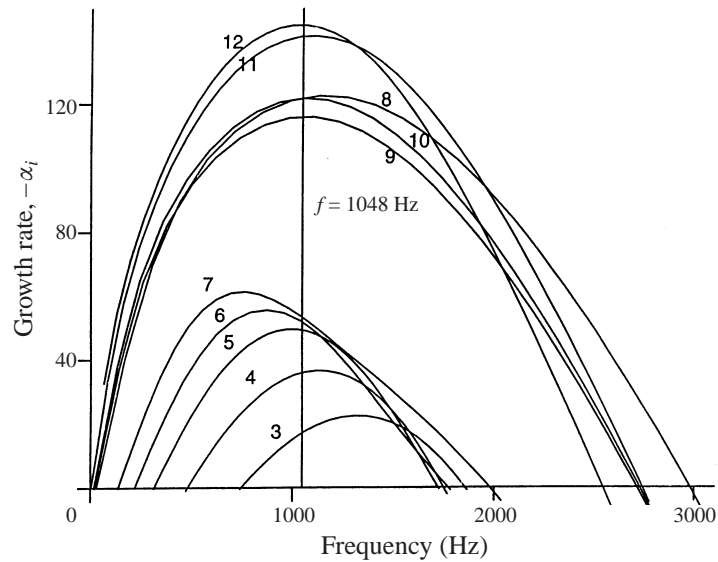


FIGURE 22. Growth rate plots for stations 3 to 12 against frequency of instability for case 1.

acoustic tone. The frequency of instability that achieved the greatest amplification between stations 1 and 12 was determined for the NACA0012 aerofoil under the flow conditions of case 1. The total amplification between the first and j th chordwise station is given by:

$$\frac{A(x_j)}{A(x_1)} = \exp \int_{x_1}^{x_j} -\alpha_i(x) dx, \quad (2)$$

$A(x_j)$ = amplitude of instability at j th chordwise station; $A(x_1)$ = amplitude of instability at first chordwise station ($x/c = 0.28$); $-\alpha_i$ = Growth rate of instability.

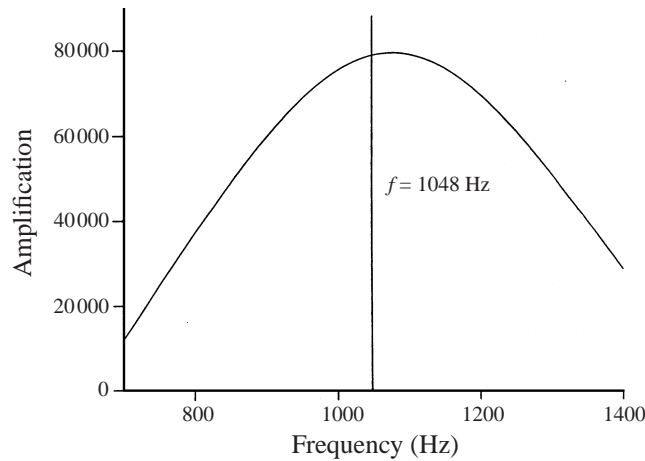


FIGURE 23. The amplification of fixed frequency modes from stations 1 to 12 for case 1.

The amplification of modes with fixed frequency was calculated over a range of frequencies. For case 1, figure 23 shows that the most amplified frequency over the aerofoil pressure surface is approximately 1050 Hz, which is very close to the experimentally obtained frequency of 1048 Hz and shows that the acoustic tone is predicted well by the frequency of the most amplified linear mode over the aerofoil. Figure 24 shows the amplification of the instability at 1048 Hz along the pressure surface of the NACA0012 aerofoil for case 1 up to station 12. It is shown that almost all of the growth of the boundary-layer instability occurs in the last few centimetres of the aerofoil, corresponding to the increased growth rate plots of figure 22.

From figure 22, it can be seen that the observed acoustic tone for case 1 bounded by the maximum growth rate frequencies before (station 7) and after (station 8) the change in structure of the growth rate curves. This change corresponds to the change from essentially T-S type instabilities to Rayleigh inflexional type instabilities. Similar results were obtained for a number of other cases investigated. From this, it is inferred that the frequency of the acoustic tone generated by the aerofoils is selected in the linear regime close to the region where the change in structure of the neutral instability curves occurs. This is confirmed by the experimental data which show that once a dominant instability frequency is selected near the point of separation, it is maintained as the most dominant instability frequency up to the trailing edge.

Linear instability analysis was conducted on the flow over the pressure surface of the NACA0012 aerofoil, for case 2, for which no acoustic tone was observed. It was shown in figure 14(a) and 14(b) that there was no large-scale amplified boundary-layer instability within the flow for this case. Figure 25 shows the growth rate plots for the stations along the aerofoil pressure surface and figure 26 shows the corresponding plot of the most amplified frequency of instability at the aerofoil trailing edge. The amplification is reduced by a factor of more than 20 over case 1 and is over a smaller band of frequencies. It can be seen that the most unstable frequency predicted to occur at the aerofoil trailing edge is 150 Hz. Case 1, for which tonal noise was observed, reaches transition at the aerofoil trailing edge, indicating massive growth of instabilities, whereas for case 2 the flow at the trailing edge is far from transitional, indicating a low growth of instabilities. The total amplification of the instability at 150 Hz for case 2 is approximately 3500 which is significantly lower than the amplification of the most amplified instability for the previous NACA0012 cases. It is believed that

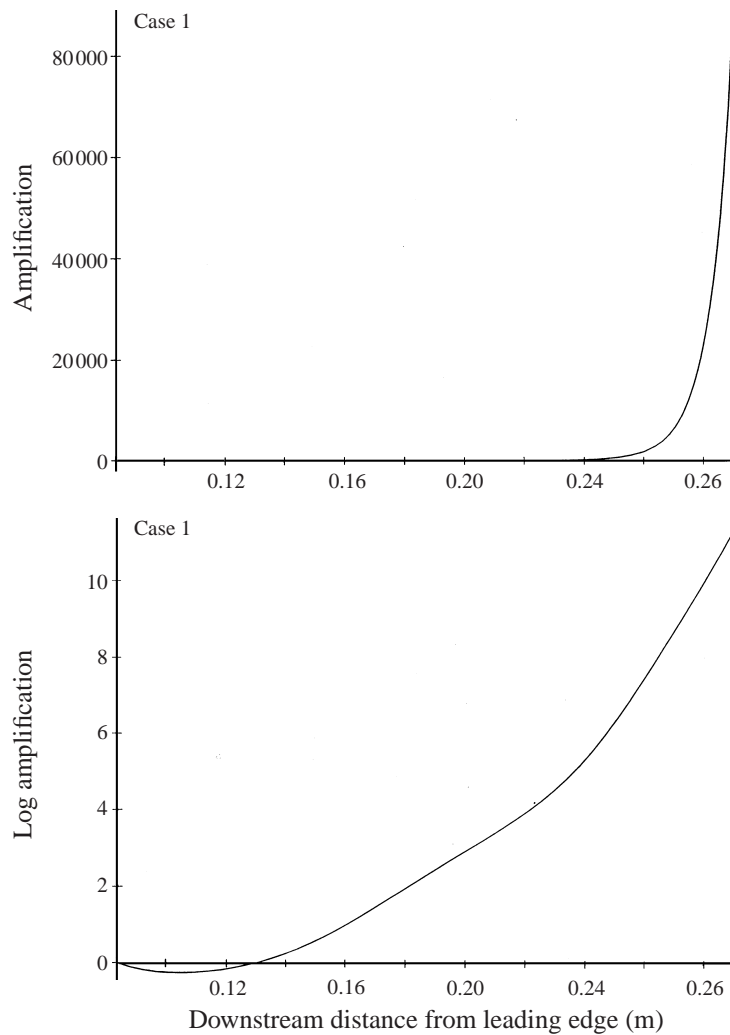


FIGURE 24. Amplification against downstream distance of the fixed frequency mode.

no large-scale amplified instability is observed in the flow for case 2 because one or more components of the feedback-loop mechanism are missing. It is suggested that the amplification is not sufficient to initiate the tonal noise mechanism.

7. A revised mechanism for tonal noise generation on aerofoils

A revised mechanism for tonal noise generation has been proposed as a result of a detailed experimental and theoretical investigation into the fundamental behaviour of the pressure surface boundary layer and mean flow around an aerofoil and combines many of the concepts from previous work. Paterson *et al.* (1973) attributed tonal noise to vortex shedding from the aerofoil trailing edge, but provided no physical basis for this argument. Subsequently, the noise was proposed to be due to a feedback-loop mechanism between T-S waves on the aerofoil pressure surface and an acoustic field generated from the trailing edge (Wright 1976; Longhouse 1977; Fink 1978; Arbey

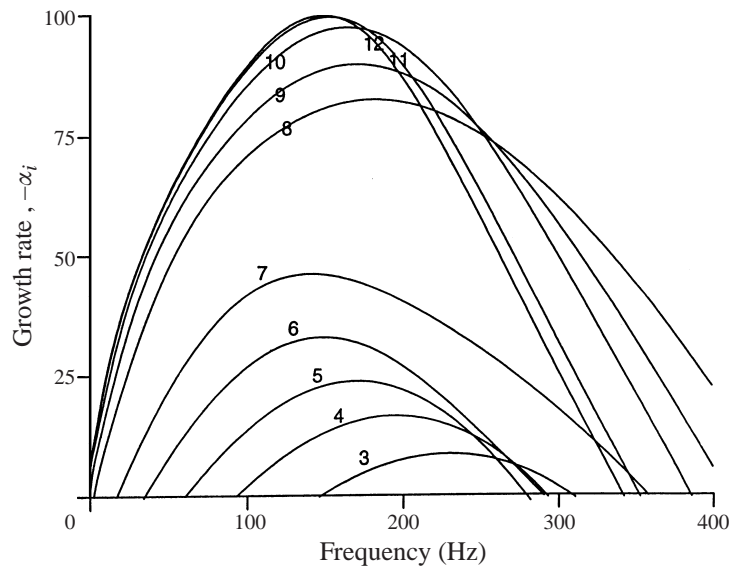


FIGURE 25. Growth rate plots for stations 3 to 12 against frequency of instability on the NACA0012 aerofoil for case 2.

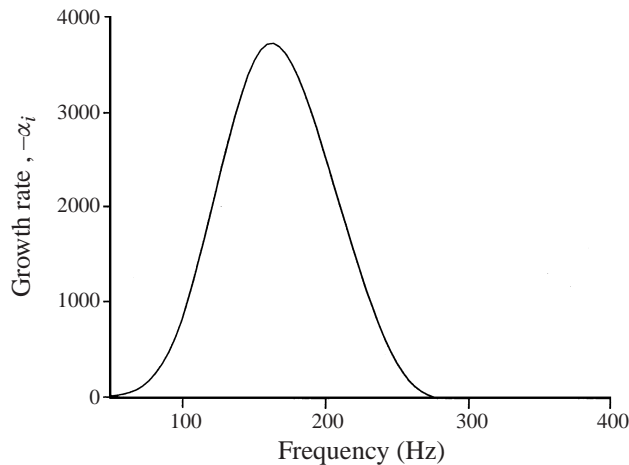


FIGURE 26. The amplification of fixed frequency modes from stations 1 to 12 for case 2.

& Bataille 1983). The frequency of the acoustic tone was believed to be that of the most amplified frequency of instability at the aerofoil trailing edge.

The new proposed mechanism is based on a vortex-shedding process, but attributes the vortex street observed to massively amplified T-S instability waves by the separating flow. An adverse pressure gradient on the pressure surface of an aerofoil leads to a region of flow with inflectional velocity profiles which develop into fully separated flow close to the trailing edge of the aerofoil. The majority of the growth of the boundary-layer instabilities occurs in these regions. The frequency of the T-S wave which is massively amplified appears to be close to the frequency of the linear mode with maximum amplification between stations 1 and 12 on the aerofoil.

This discrete instability frequency continues to amplify as it propagates towards

the trailing edge of the aerofoil and begins to roll up into a vortex. The interaction of this rolled up instability with the trailing edge of the aerofoil results in a scattered oscillating field around the aerofoil that oscillates at the same frequency as the most amplified instability. This oscillating field extends upstream to approximately 50 % chord which is close to the point at which the discrete frequency instability becomes unstable. It is hypothesized that the oscillating mean flow provides an upstream feedback mechanism for selection of the most amplified instability, resulting in the extremely narrow-band acoustic tone observed.

It will be appreciated that the model presented depends on inviscid amplification by inflexional velocity profiles rather than by separation *per se*. More detailed studies (Nash 1996) have shown that, although separation is the most usual cause of the amplification, it is not universal. Discrete tone generation was observed in cases where no absolutely reversed flow was detected, but where there were nevertheless inflexions in the measured velocity profile.

A damping mechanism is a necessary part of the overall process. The considerable amplitude of the peak tones relative to the background level, and the strong frequency selectivity show that damping is low. Damping seems likely to be controlled by viscous processes within the intensely fluctuating velocity field, although the loss of energy via radiated sound will also contribute, especially at higher velocities.

In nearly all previous work on aerofoil tones, notably the original work by Paterson *et al.*, a ladder frequency response was observed. This has been studied by several writers, who have all suggested that some form of instability loop will be present, and be a key feature of the process. The current experiments, and the present theory, have shown that there is no necessity for a ladder process to occur in order for substantial acoustic tones to be present. The tones can be explained purely in terms of the amplification of the classic T-S instabilities within the boundary layer, and separating shear layer.

It is noteworthy that earlier results from the present work in a hard-wall tunnel reported by Lawson *et al.* (1994) and shown here in figure 4, did demonstrate a ladder frequency response, but this was eliminated by the provision of acoustic lining around the aerofoil. It is thought that the existence of a feedback loop will have its essential consequence in changing the nature of the starting conditions for the T-S instability process. Thus, it should be possible to compute such instabilities around the loop.

8. Conclusions

Intense narrow-band tones, up to 40 dB above background noise levels, have been found on a variety of aerofoils tested at modest Re and angle of attack, provided that the flow and surface finish are adequate to promote laminar flow. The complex frequencies generated by the aerofoil were found to be highly repeatable. The frequency range and structure of the tones generally compared well with those measured by Paterson *et al.* (1973).

The structure of the tones was heavily influenced by the resonances with the wind-tunnel walls. A quasi-anechoic environment designed to minimize acoustic feedback processes eliminated the complex tone structure.

Advanced LDA techniques have been used to obtain detailed measurements of mean and r.m.s. velocity fluctuation profiles as well as spectral and cross-spectral measurements. The 3-component LDA has proved to be an extremely powerful tool in enabling high resolution, directionally unambiguous measurements to be taken non-intrusively within unsteady reversed flow. These measurements have revealed the

presence of massively amplified boundary-layer instabilities at the pressure surface trailing edge. Flow visualization showed that these instabilities roll up into a regular von Kármán vortex street which is shed at the frequency of the acoustic tone. Both the appearance of these massively amplified instabilities and the subsequent acoustic field was found to be highly correlated with the region of pressure surface trailing edge separated flow. A large-scale scattered oscillating mean flow was found to exist around the aerofoil in the presence of tonal noise. This scattered field oscillated at the frequency of the acoustic tone and was found to extend upstream from the trailing edge to approximately 50 % chord and into the wake. This flow did not satisfy the unsteady Kutta condition.

Theoretical modelling of boundary-layer instability characteristics revealed that the frequency of the acoustic tone generated by the aerofoils could be predicted using linear stability theory. The frequency is selected as that with the maximum total amplification close to the region where inflectional instabilities begin. On the basis of both the experimental and theoretical work described, the generation of acoustic tones has been shown to be dependent on the presence of trailing-edge separating flow. A new mechanism of tonal noise generation on a two-dimensional aerofoil has been proposed based on amplification of T-S waves by a separating laminar shear layer near the trailing edge of the aerofoil.

This work was supported under grants from the EPSRC. The help of Professor P. G. Drazin throughout the work is warmly acknowledged.

REFERENCES

- AIZIN, L. B. 1992 Sound generation by a Tollmien–Schlichting wave at the end of a plate in a flow. *Prikl. Mekh. Tekh. Fiz.* **3**, 50–57.
- AKISHITA, S. 1986 Tone-like noise from an isolated two dimensional aerofoil. *AIAA paper* 86–1947.
- ARBET, H. & BATAILLE, J. 1983 Noise generated by airfoil profiles placed in a uniform laminar flow. *J. Fluid Mech.* **134**, 33–47.
- ARCHIBALD, F. S. 1975a The laminar boundary layer instability excitation of an acoustic resonance. *J. Sound Vib.* **38**, 387–402.
- ARCHIBALD, F. S. 1975b Unsteady Kutta condition at high values of the reduced frequency parameter. *J. Aircraft* **12**, 545–550.
- BARRETT, R. V. 1984 Design and performance of a new low turbulence wind tunnel at Bristol University. *Aeronaut. J.* **88**, 86–90.
- BARRETT, R. V. & SWALES, C. S. 1998 Realisation of the full potential of the laser Doppler anemometer in the analysis of complex flows. *Aeronaut. J.* **102**, 313–320.
- BROOKS, T. F., POPE, D. S. & MARCOLINI, M. A. 1989 Airfoil self noise and prediction. *NASA Ref. Pub.* 1218.
- CLARK, L. T. 1971 The radiation of sound from an airfoil immersed in a laminar flow. *Trans ASME A: J. Engng Power* **93**, 366–376.
- DJENIDI, L. & ANTONIA, R. A. 1995 *LDA Measurements: Power Spectra Estimation*. Dantec Information 14.
- DOVGAL, A. V. 1985 Development of Vortical Disturbances in Flow with Laminar Separation. *Proc. IUTAM Symp. Laminar–Turbulent Transition*, pp. 359–366, Springer.
- DOVGAL, A. V. & KOZLOV, V. V. 1983 Influence of acoustic perturbations on the flow structure in a boundary layer with adverse pressure gradient. *Fluid Dyn.* **18**, 205–209 (trans. from Russian).
- DOVGAL, A. V., KOZLOV, V. V. & MICHALKE, A. 1994 Laminar boundary layer separation: instability and associated phenomena. *Prog. Aerospace Sci.* **30**, 61–94.
- FALKNER, V. M. & SKAN, S. W. 1931 Some approximate solutions of the boundary layer equations. *Phil. Mag.* **12**, 865.
- FFOWCS WILLIAMS, J. E. & HALL, L. H. 1970 Aerodynamic sound generation by turbulent flow in the vicinity of a scattering half plane. *J. Fluid Mech.* **40**, 657–670.

- FINK, M. R. 1978 Fine structure of airfoil tone frequency. Paper H3 presented at the 95th Meeting Acoust. Soc. Amer.
- FINK, M. R., SCHLINKER, R. H. & AMIET, R. K. 1976 Prediction of rotating-blade vortex noise from noise of non-rotating blades. NASA CR-2611.
- FREYMUTH, P. 1989 Air flow visualization using titanium tetrachloride. *Lecture Notes in Engineering, Adv. Fluid Mech.* (ed. M. Gad-el-Hak).
- GASTER, M. 1966 The structure and behaviour of laminar separation bubbles. *AGARD Conf. Proc.* **4**, *Separated Flows*, 813–854.
- HAMA, F. R. 1962 Streaklines in perturbed shear flow. *Phys. Fluids* **5**, 644–650.
- HARTREE, D. R. 1937 On an equation occurring in Falkner and Skans's approximate treatment of the equations of the boundary layer. *Proc. Camb. Phil. Soc.* **33**, 223.
- HERSH, A. S. & HAYDEN, R. E. 1971 Aerodynamic sound radiation from lifting surfaces with and without leading-edge serrations. NASA CR-114370.
- HOWARD, F. 1987 *Wilbur and Orville—A Biography of the Wright Brothers*. Alfred A. Knopf.
- LIN, C. C. 1995 *The Theory of Hydrodynamic Stability*. Cambridge University Press.
- LONGHOUSE, R. E. 1977 Vortex shedding of low tip speed, axial flow fans. *J. Sound Vib.* **53**, 25–46.
- LOWSON, M. V., FIDDES, S. P. & NASH, E. C. 1994 Laminar boundary layer aeroacoustic instabilities. *AIAA Paper* 94-0358, 32nd Aerospace Sciences Meeting and Exhibition, Reno.
- MCALPINE, A. 1997 Generation of discrete frequency tones by the flow around an aerofoil. PhD thesis, School of Mathematics, University of Bristol.
- MCALPINE, A., NASH, E. C. & LOWSON, M. V. 1999 On the generation of discrete frequency tones by the flow around an aerofoil. *J. Sound Vib.* (to be published).
- MUNIN, A. G., PROZOROV, A. G. & TOPOROV, A. V. 1992 Experimental study of noise generated in a low-velocity flow. *Sov. Phys. Acoust.* **38**, Jan–Feb. 1992.
- NASH, E. C. 1996 Boundary layer instability noise on aerofoils. PhD thesis, Department of Aerospace Engineering, University of Bristol.
- NASH, E. C. & LOWSON, M. V. 1995 Noise due to boundary layer instabilities. *Paper CEAS/AIAA-95-124*, CEAS/AIAA Aeroacoustics Conference, Munich.
- PARKER, R. 1996 Resonance effects in wake shedding from parallel plates: Some experimental observations. *J. Sound Vib.* **4**, 62–72.
- PARKER, R. 1997 Resonance effects in wake shedding from parallel plates: calculation of resonant frequencies. *J. Sound Vib.* **5**, 330–343.
- PATERSON, R., VOGT, P., FINK, M. & MUNCH, C. 1973 Vortex noise of isolated airfoils. *J. Aircraft* **10**, 296–302.
- SCHLINKER, R. H., FINK, M. R. & AMIET, R. K. 1976 Vortex noise from non-rotating cylinders and airfoils. *AIAA Conf. Paper* 76-81.
- SHEN, S. F. 1954 Calculated amplified oscillations in the plane Poiseuille and Blasius flows. *J. Aeronaut. Sci.* Readers Forum, 62–64.
- SOINNE, E. & LAINE, S. 1988 An inverse boundary element method for single component aircraft design. *J. Aircraft* **22**, 541–543.
- SUNYACH, M., ARBEY, H., ROBERT, D., BATAILLE, J. & COMTE-BELLOT, G. 1973 Correlations between far field acoustic pressure and flow characteristics for a single airfoil. *AGARD Conf. Proc.* **131**, Noise Mechanisms, Paper 5.
- SWALES, C. 1994 Advanced LDA techniques for measurement of 3D boundary layer velocity profiles on a helicopter rotor. PhD thesis, Bristol University.
- SWALES, C., RICKARDS, J., BRAKE, C. J. & BARRETT, R. V. 1993 Development of a pin-hole meter for aligning 3-D laser Doppler anemometers. Dantec Information no. 12.
- TAM, C. K. W. 1974 Discrete tones of isolated airfoils. *J. Acoust. Soc. Am.* **55**, 6.
- WRIGHT, S. E. 1976 The acoustic spectrum of axial flow machines. *J. Sound Vib.* **45**, 165–223.